ADDIS ABABA UNIVERSITY

SCHOOL OF GRADUATE STUDIES

VELOCITY STRUCTURE OF THE UPPER CRUST ACROSS THE MAIN ETHIOPIAN RIFT

MEHARI MELAK

JUNE 2004

ADDIS ABABA UNIVERSITY
SCHOOL OF GRADUATE STUDIES
FACULTY OF SCIENCE
DEPARTMENT OF GEOLOGY AND GEOPHYSICS

VELOCITY STRUCTURE OF THE UPPER CRUST ACROSS THE MAIN ETHIOPIAN RIFT

A THESIS SUBMITTED TO THE SCHOOL OF GRADUATE STUDIES IN PARTIAL FULFILLMENT OF THE REQUIRMENT FOR THE DEGREE OF MASTER OF SCIENCE IN GEOPHYSICS.

BY:- MEHARI MELAK

JUNE 2004

ADDIS ABABA UNIVERSITY
SCHOOL OF GRADUATE STUDIES

VELOCITY STRUCTURE OF THE UPPER CRUST ACROSS THE MAIN ETHIOPIAN RIFT

BY: -

MEHARI MELAK
FACULITY OF SCIENCE
GEOLOGY AND GEOPHYSICS
DEPARTMENT

APPROVED BY BOARD OF EXAMINERS: -

Dr. Dereje Ayalew _____

Chairman

Dr. Tilahun Mammo _____

Advisor

Ato Befekadu Oluma _____

Examiner

Ato Ketsela Tadesse _____

Examiner

ACKNOWLEDGEMENTS

First and foremost I would like to thank the Almighty **God** for everything he did for me.

A profound gratitude is expressed to my advisor **Dr. Tilahun Mammo** for his uncountable effort in bringing the data from the Ethiopian Afar Geoscientfic Lithospheric Experiment (EAGLE) project; and for his proper guidance, valuable advice, material help and in giving comments and correcting the thesis.

I am very grateful to **Dr. Tenalem Ayenew**, Dr, Tigistu Haile and Dr. Mohammed Umer for their various help and assistances.

My deepest heart-felt gratitude goes to my teaching staffs at Bole High school, for conducive environment they created for me through out my studies. Special thanks goes to **Ato Belayneh Debalke** (Vise director school) for his moral building advice and material help.

I thank all the member of my family in their everyday encouragement, support and love. My deepest appreciation goes to my dearest Netsanet Yeshitela for her economical help.

I offer My exceptional thanks to **Bekele T amirat**, Bekele Asefa, Girma Mengistu, Takele Wakjira,Getachew Abera, Sinkinesh Beyene,Yeshambel Abebe, Degena Bezabeh,Gezahegn Debebe, **Mahlet Teferawork** and all my friends who gave various assistances through out the work.

Finally I would like to express my heart-felt gratitude and love to my colleagues and batches **Ali Ahmed** and Tesfay Hailu for creating conducive and collaborative environment throughout the study time.

THANKS

Table of contents

List of figures

List of tables

ABSTRACT

Refraction technique is one of the geophysical investigation methods used to map the subsurface layers based upon the velocity variation of the seismic wave as it propagates through different geological materials.

As a part of the Ethiopia Afar Geoscientfic Lithospheric Experiment (EAGLE) project conducted in January 2003, the detail study of the crustal seismic P-waves has been carried out to produce the seismic model down to the depth of 10 km from Chefedonsa (E513296, N9926410 to Kula (E575823, N886441) for about 120Km profile length across the Main Ethiopian Rift.

Five shot points with inter shot separation of about 46Km were used as seismic source and the data were recorded on 120 geophones deployed in the study area at 1 km spacing.

The first arrival times were picked, processed and inverted using the generalized reciprocal method (GRM); and gave the four major seismic layers up to the depth of 10 km across the rift.

There is a steady increase in P-wave velocity from about 3000m/s in the first layer to about 6365m/s in the last layer. Lateral Velocity variations are also observed in the layers.

Attempts have been made to correlate the seismic layers with the known geological formations. Boarder faults and other major faults have been clearly identified.

CHAPTER-1

INTRODUCTION

1.1. LOCATION AND GEOLOGICAL SETTING OF THE STUDY AREA

The study area, as it is shown in fig.1 crosses the Main Ethiopian rift. It is from Chefedonsa (8°, 98'N; 39°, 12'E) through Doni to Kula (8°, 12''N; 39°, 69"E).

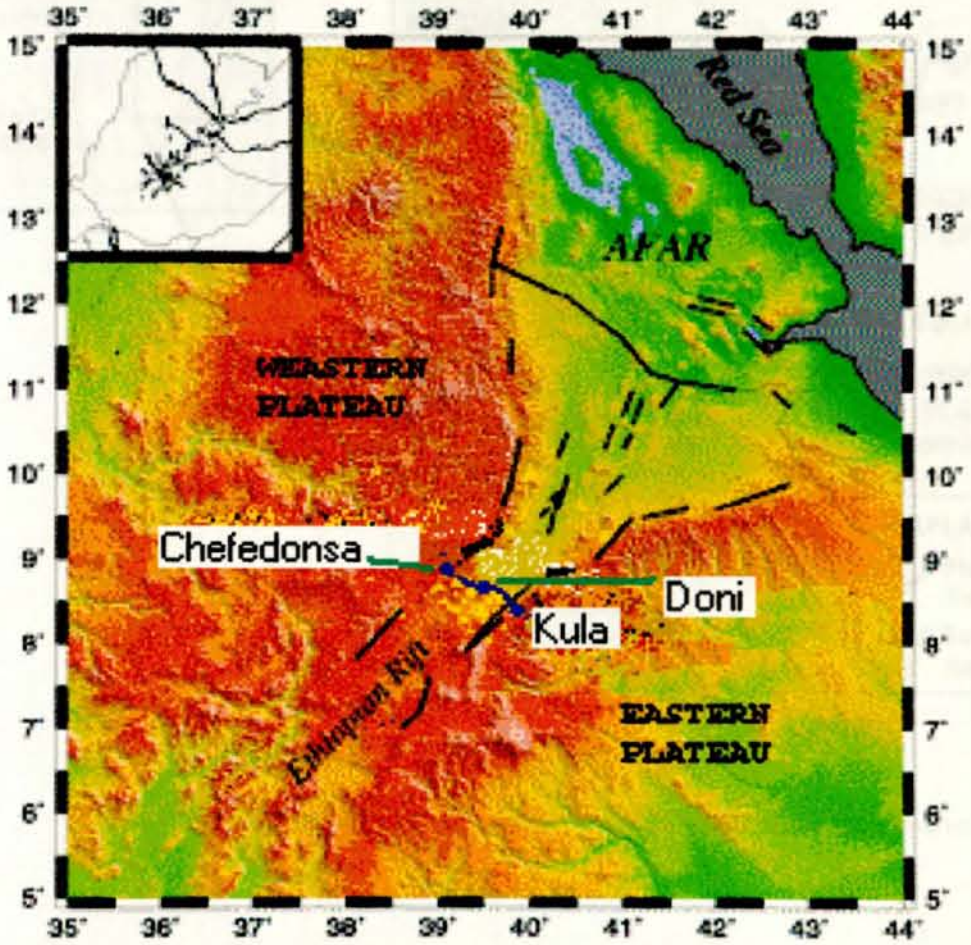

Fig1. Map of the study area

● Shot points

Study profile

The Main Ethiopia Rift valley is a part of the African Continental Rift system, which consists of a series of rift zones (Rosemdaht et al, 1986) and extends for 3200 km from the Afar triple junction at the Red sea-Gulf of Aden intersection to the Zambezi River in Mozambique. (Fig-2)

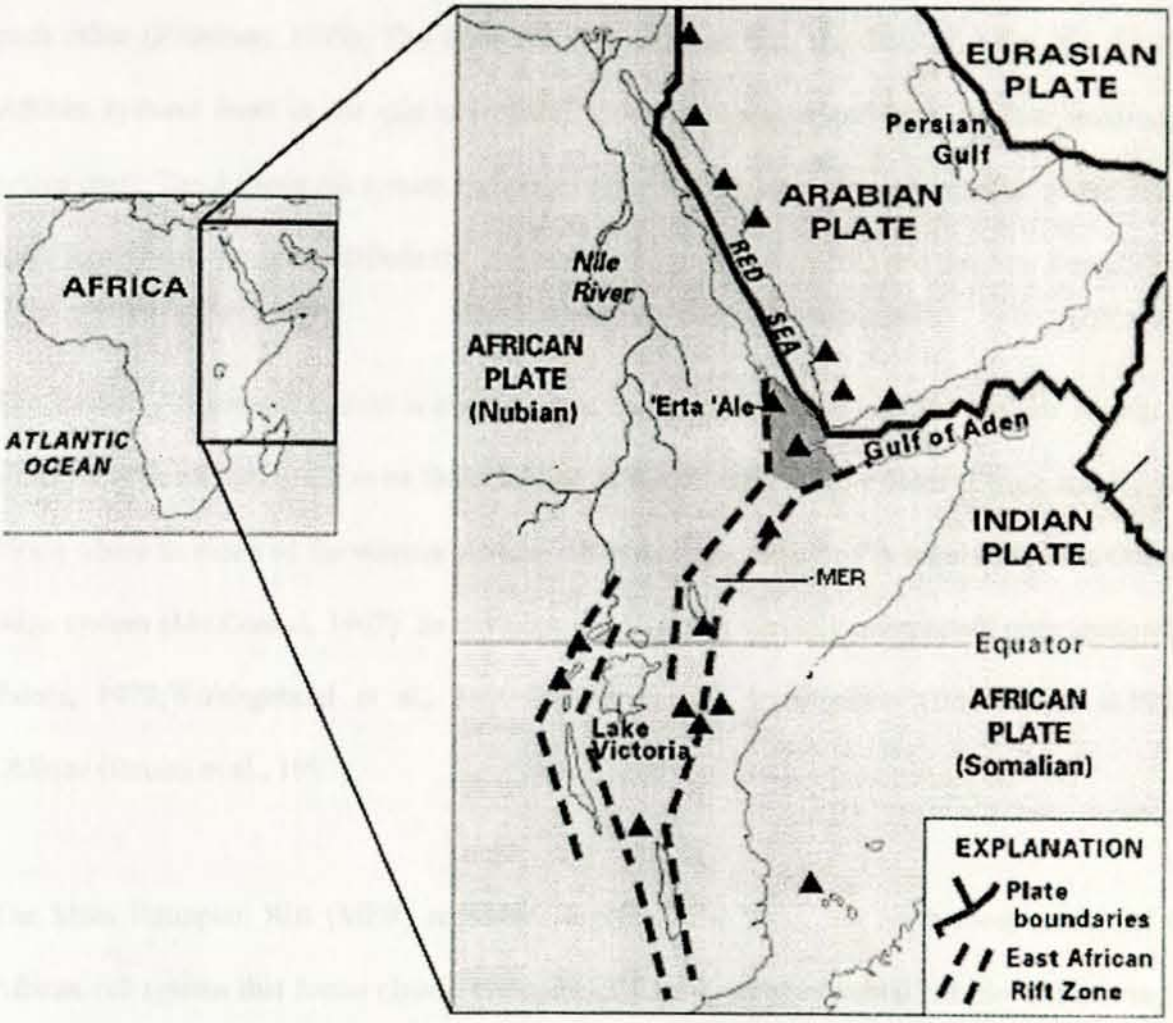

Fig-2. The East African rift system (The triangles are historically active volcanoes.)

Rifting in northeastern Africa started some 30million years ago when the earth's crust uplifted by a lithothermal system of forces (Gass, 1970a, b) generated by a stationary hot spot in the

underlying mantle (Burek, 1975). The three radial rifts developed due to radial flow from the top of the mantle plume. The red-sea and the Gulf of Aden are active diverging boundaries along which the Arabian Peninsula is being separated from northeastern Africa (fig 2). The third relatively inactive, which is the north most African Rift valley, lying at an angle of about 120° to each other (Plummer, 1999). The three rift systems: Red sea, the Gulf of Aden and the East African systems meet in the afar depression which is characterized by a shallow tectonically active crust. The African rift system comprises several units, the most important of which are the Lake Rudolf rift, the Lake Stefanie rift, the Main Ethiopian Rift (MER) and the Afar Depression.

The Eastern African rift system is characterized by abundant volcanism and shallow earthquake which may be an indication to be the extension of the Oceanic ridge system (Ewing and Heezen, 1956) where as much of the western African rift system are older and is unrelated to the Oceanic ridge system (Mc.Connel, 1967). Its development has been variedly interpreted, pure tension (Di Palola, 1972;Woldegebriel et al., 1990;Ebinger et al.), transtension (Boccalettiet al.1992), Oblique (Bonini et al., 1997)

The Main Ethiopian Rift (MER) represents together with Afar, the north most section of the African rift system that forms classic examples of young intercontinental rift. So that a string of ten major volcanic centers runs the length of the Ethiopian rift. These silicic centers have been initiated and active within the late Pliocene, Holocene interval, and the resulting lava ignimbrite shields are generally well-preserved appreciable local erosion and lacustrin deposition during the Pleistocene pluvial periods, Mohr, 1990. Further south the Main Ethiopian Rift transects the Ethiopian dome separating the country in to two major blocks -the Nubian plate to the west from

the Somalia plate in the east. This rift is slowly widening to become Ocean-meet with the major geological features on the earth, the east African rift Valley. In time the African plate will split apart along the line of the Ethiopian dome and form a new Ocean (Ethiopian Afar Geoscientfic Lithosperic Experiment, 2003)

The Main Ethiopian Rift which is NNE striking having a width of 10 to 80km. extends for about 650km.from the Lake Chamo region in the south (4° 45″) to the region of Ayelu volcano in the north (9°, 45″) beyond which its NNE trending structure are replaced by the NNW trending structure of the Afar depression with out significant break. .Mohr, 1967; Wolde, 1989). The MER system has been evolving over the past 43 Ma (Levitte et al., 1074;Davidson and Rex, 1980;Morton et al.,1979) and according to Kazmin et al,(1980) there were major episodes of rifting at 10, 5, 4 and 1.8-1.6 Ma. Each stage of rifting and down falling was accompanied by a bimodal (silicic-mafic) volcanism in the rift and formation of basaltic and trachytic shield volcanoes on the rift shoulder and margins (Tefera.,Chernet and Haro,1996).The development of the MER is accepted to be due to the drifting apart of the western plateau to the western and the eastern plateau to the east through tensional faulting.

Eruption of huge volumes of volcanities started in the MER and the adjacent plateaus in late Eocene Early Oligocene (Merla et al., 1979; Kazmin et al.1980, Zanettin, 1993), preceding rift formation. The most important Volcano-tectonic event in the central sector of the MER occurred in Early Pliocene, with the eruption of voluminous flow of rhyolitic ignimbrites and the collapse of very large calderas (Di paola, 1972). From Early Pleistocene to the present tectonic and volcanic activity was concentrated along the Wonj Fault Belt WFB and successively along the

Silti-Debrezeit Fault Zone SDFZ (Mohr, 1962; Di Paola, 1972; Bigazzi et al., 1993). Quaternary volcanism, faulting, tensional fissures on a hard rock, earthquake catalogue of the region and geodetically measure extension rates have been the main indicators of the tectonic activity in te east African rift. The seismicity studies in Ethiopia and the adjacent areas confirm that this fault system is still developing. Most of the rocks exposed along the Ethiopian rift is mainly covered by Quarternary basaltic, trachytic and rhyolitic lavas,pyroclastics flows and fall deposits, and volcanic clastics sediments(Korme,1997).The WFB comprises three en-echelon,NNE-trending segments with in the rift Lakes basin (Mohr,1960;Lloyd,1977) named from south to north the Corbetti-Shalla,Shalla-Ziway and east Ziway segments.

The western plateau shows a very gentle decline westwards towards the prominent escarpment overlooking the sudden plains. According to Kazmin et.al.,1975,it is occupied with less dominant Mesozoic sedimentary rocks, which belongs to Antalo group and Amba Aradom formation, and the dominant Cenozoic rocks. Also it is intercepted with huge Miocene volcanic ranges and created cones that decline from north to south and lying plateau level; the high peaks are north of blue Nile (Ras Dashen , 4550m).The plateau Trap series of early and middle Tertiary age are exposed in the western escarpment and consists of about 1000m of basaltic lava flows, with interbeded ignimbrite beds, topped by massive rhyolites and intervening tuffs and basalts (Di Paola, 1972,1993;Merla et al.1979)

The Pliocene ignimbrites, like the Trap series basalts, are thickest along the western margin of the rift system, having erupted from a line of fairly well preserved centers that may mark the site of a

fissure (Mohr, 1967). Pleistocene Aden series basalts are found generally in small amount but numerous patches on the plateaux, the eruption having been from small lava cones (Mohr, 1967).

The eastern plateau has an average elevation covered by Pliocene to early Pleistocene shield volcanoes (Chilalo,4005m; Kecha,4245m; Badda,4170m). These consist of trachytes with subordinate basalt and mugearites.(Di Paola,1972;Merla et al.,1979).The eastern escarpment is strongly up wards in the chain of the rift lakes ,lake Ziway and lake Langano. This strongly stepped escarpment is formed by complex of NNW trending Pleistocene faults (Abera, 1990).

The central sector of the MER consists the five large rift lakes of tectonic or volcanic tectonic origins. These are Ziway, Langano, Abyata Shala and Awasa lakes MER and its shoulder are made of Silicic pyroclastic materials (Mohr, 1962,Di Paola, 1972), they are early middle Pliocene (Woldegebriel et al.1972). The thick section of rhyolites, ignimbrites,interlayered with basalts and unwelded tuffs and ash flows and trachytes commonly named as Nazret Groups form the large part of the rift floor and also outcrop in some part of the rift and escarpments and the adjacent plateau margins.(Kazmin,1978) Where as large areas of the rift floor covered by volcanic lacustrine and fluvial lacustrine deposits (Benvenuti & Balewald, 2002). Along the eastern margin of the rift the Alaji basalt are conformably overlapped by a unit of flood basalts and siliceous rocks which in turn overlapped with slight unconformity by silicic volcanics of the Nazret Group(Kazmin& Berhe,1978).

In the MER Aden series basalts are rather rare. The most notable occurrence is north –west of lake margarita, east of lake Ziway, and, along the foot of the Gouraghe horst extending

northwards. Pleistocene silicic lavas and ignimbrites are significantly restricted to the WEB of the rift system (Mohr, 1967).

The floor of the rift rises about 600m from north to south, reaching maximum elevation of 1800m in the Meki watershed. Fragmentation of the rift floor formed the youngest structural deformation largely concentrated in a narrow 5-12 km wide belt of normal faults, known as the Wonji Fault Belt (Mohr et al., 1980;Lioyd, 1977). WFB has a NNE orientation along the rift margin envelope (Mohr, 1 980) P leistocene s ilicic l avas a nd i gnimbrites are significantly restricted to the Wonji Fault Belt of the rift system. The silicic centers occur as fairly large cones, frequently manifesting simple or compound calderas. The cones are composed of silicic lavas,ignimbrites and pumice flows(Gibson,1967b;Mohr,1962b,1966b). Some of the latest lavas of the WFB silicic are of Holocene age, in particular associated with calderas of Fantale (Mohr,1967).

1.2. LITHOLOGICAL UNITS OF THE STUDY AREA

The Geology of the area was studied by several researchers (Mohr, 1961;Jusentin, 1974;Kazmin & Berhe, 1978;Girmay & Assefa, 1989; Boccaletti and Assefa, 1975;Mazzarini & Abebe, 1999;Wolde, 1996, and others). Their study is summarized as follows.

1.2.1. Intra rift complex

The upper Miocene-Quaternary products constitute the floor of the main rift and its successive filling is taken as rift comlex.

The first group of this comlex forming the floor of the rift is the Nazret group. The lithologicl units of the Nazret group are welded ignimbrite with fiamme,pumice,ash and rhyolite flows in MER rift margins and adjacent plateaus (Kazmin and Berhe,1978). In the rift floor its thickness is 200-250m and tends to thin out on the escarpments. In composition the ignimbrites are sub-alkaline rhyolites and trachytes with rare peralkaline varieties. This unit comprises also numerous rhyolitic (Abadi,Ruketi,Aminos) and trachytic domes (Gara B okan,Dikub),which a re d ifferent formations with age ranging from about 7 to 3 Ma.(Mohr,1971;Zanettin & Justin-Visentin,1974)

The other unit which out crop along the border of the central plain is the Chefedonsa Unit (Mazzarini, 1999). It consists of fall deposits and poorly welded ignimbrites of rhyolitic composition. The Chefedonsa unit rests up on the Addis Ababa basalt and lacusterine deposit in the south western and covered by the Nazret group in the eastern and northeastern areas. The total thickness of the unit varies from few meters to 40m close to the Chefedonsa village, where the most complete section exposed. Fission track Analysis in a section close to Chefedonsa village yielded an age of 2.2Ma. (Mazzarini, 1999).

1.2.2. Rift Axis complex

It includes the Quaternary-Holocene sequence of the young central volcanoes,lacustrine deposits and basaltic cinder and spatter cones. This sequence presents the same volcanic and structural features recognized in the younger sequence of the adjacent MER (Kazmin & Behre,1978). The different units in this complex are:-

Zikwala Volcanic unit:- This unit is an isolated well preserved composite cone. Lavas are the dominant products, with pyroclastic mainly occurring at the foot of the volcano. The lavas of this unit are composed of Peralkaline trachytes, which are, generally, anorthoclase-phyric. Radiometric ages range from 1.3Ma to 0.85Ma.

Bishoftu Volcanic unit: - This unit forms a NNE trending belt out cropping mainly in the eastern flat area of Debrezeyt. It is also known as Wonji basalts. The two groups of this unit are the spatter and cinder cones with associated tabular lavas and the phreatomagmatic deposit. The latter consisting mainly of surges and highly fragmented deposits with maars and tuff rings.

Bofa Basalt:- Bofa basalts are well developed in the northern and central part of the MER. The lower age limit of 3.5Ma has been reported by Kazmin et al., 1980b. This basalt is olivine, mostly aphyric Pliocene flood basalt known by different name in different localities, Welenchiti basalt (Meyer et al., 1975), Bishoftu basalts and rhyolities(Zanettin and Justin,1974) old rift floor basalt(U.N..gothermal project,1972).

1.3. THE CROSS RIFT LINEAMENTS

The MER in particular shows isolated cross-rift lineament as a separating line (Mohr, 1967). The displacements of the plateau-rift margins are along the cross-rift lineaments of the Ethiopia rift system. The cross-rift lineament trend WNW-ESE in the MER that are remarkable for their linearity and their persistence over long distances.

The dense swarms of NNE_SSW trending steep normal faults, still active on the margins along the Silti-Debrezeit Fault Zone (SDFZ) on the west and the Wonje Fault Belt (WFB) on the east accommodate total offsets of the rift floor and the Plateaus (Di Paola, 1972;Woldegebriel et al.1990) WFB at the floor of the MER is marked by the persistent belt of intense, fresh faulting has dextral displacement. The faults are short and normal type and are notably associated with tensional fissures (Gibson, 1967b). The WFB is frequently, but not always, axial to the rift and is dextrally displaced along the same cross-rift lineaments that displaced the rift margins. It is a line along which recent lavas and ignimbrites have erupted, and the whole tectonic association of crustal tension acting across the rift (Mohr.1967a). The silicic centers of the WFB are situated where there is an intersection from a cross-lineament, and their calderas or craters are elongated in the direction of the cross-lineament.

The ESE-WNW Yerer volcanic line marks a faulted and possibly warped boundary between the plateau rocks to the north and the rift ignimbrites to the south. Most scarps can be seen to be major structural down wards in place, most can be seen to be structural down warps commonly modified by normal faulting . The relative importance of faulting and down wards varies from

place to place; that the rift margin of south of Addis Ababa is a very gentle flexure, only slightly modified by faulting where as the structure of the directly opposing rift margin near Assela is dominated by normal faulting (Mohr, 1966); with in the rift, Quaternary tensional faulting is dominant.

1.4. PURPOSE OF THE STUDY

The study area crosses the Main Ethiopian Rift that has high tectonic activity. Purpose of the studies: -

1. to identify and map the major stratigraphic units and understand its geological history.
2. to produce a cross-rift seismic model

1.5. METHDOLOGY

The methods employed inorder to achieves the objective of the research are;-

1. Seismic data are collected using 5 shots having 50 Km separation and 68 geophones having 1.74km separation on average.
2. The explosive charge type used as an energy source was powergel C^+ with primex booster and explosive cords. The recording device is Reftex Texan, a 1-channel recorder with a single 4.5hz geophone.

3. High resolution GPS were used for locating the Texans and shot point position and elevations. The topographic Map of scale 1:50,000 were used during the Texans deployment and recovery.

4. The appropriated data processing and interpretation techniques have been used to map the various seismic layers.

CHAPTER 2

THEORY

The propagation of a disturbance through a material medium is known as mechanical wave. The mechanical wave, which is also called seismic disturbance, is produced when the ground vibrates elastically either by an artificial source (explosive, weight drop....) or naturally (earthquake). The first use of an artificial energy source in a seismic experiment was in 1846 by Robert mallet, an Irish physicist. John mine introduced the drop weight as an energy source in 1885.Seismic surveys would not be possible with out sensors (geophones) to detect the returned signals. They are used to convert seismic energy in to a measurable electrical voltage.

2.1 TYPES OF SEISMIC WAVE

Seismic waves that carry tiny packet of elastic strain energy travel away from any seismic source at speeds determined by the elastic moduli and the densities of the medium through which they pass. Part of the seismic energy propagates through the body of the media as a body wave while the remaining spreads out over the surface as surface wave.

2.1.1 Body waves

There are two types of body waves, which travel through the body of an elastic medium. The first type of body wave is compressional wave. It is also known as p- wave, which is the most

important in exploration seismology .The particles of the medium oscillate about a fixed point in the direction of the wave propagation by compressional and dilatational strain.(Fig.3a)

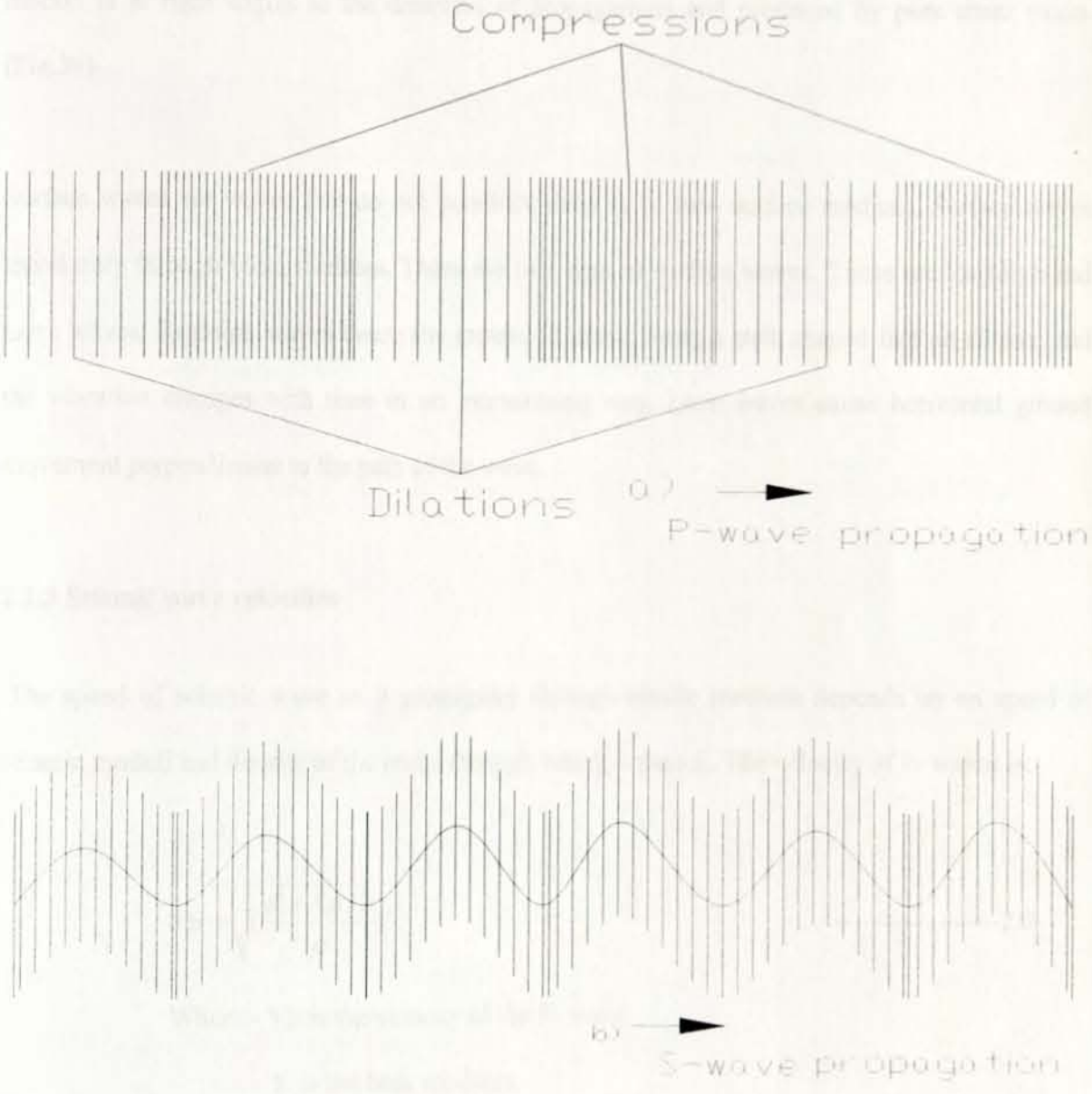

Fig.3.The propagation of seismic wave

2.1.2 Surface waves

The second type of seismic wave is transverse wave. It is also known as S- wave. The particle motion is at right angles to the direction of propagations and produced by pure shear strain. (Fig.3b)

Surface waves are waves that do not penetrate deep in to sub- surface medium. Surface waves travel only through solid medium. There are two type of surface waves. These are Rayleigh and Love waves. Rayleigh waves cause the ground to move along a path shaped like an ellipse; and the vibration changes with time in an increasesing way. Love waves cause horizontal ground movement perpendicular to the path of the wave.

2.1.3 Seismic wave velocities

The speed of seismic wave as it propagates through elastic medium depends up on speed of seismic moduli and density of the rocks through which it passes. The velocity of P- waves is.

$$Vp = \sqrt{(\frac{K + 4\mu/3}{\rho})} \qquad \text{----------2.9}$$

Where:- Vp is the velocity of the P- wave

K is the bulk modulus

μ is the shear modulus

ρ is the bulk density of the rock (material)

And velocity of S- waves is;

$$Vs = \sqrt{\frac{\mu}{\rho}} \qquad \text{----------2.10}$$

Where: - μ is shear (rigidity) modulus

ρ is the density of the medium. (Different geological materials have different density and elastic moduli.)

2.2. PRINCIPLES OF REFRACTION SEISMIC

The refraction seismic method is based on the principles of Huygens Fermat and Snells

2.2.1. Huygens' principle

The propagation of the seismic wave through an earth material is determined by the advancement of the wave front Christian Huygens', 1678; first explained this in his principle that stated 'all points on a wave front can be regarded as point sources for production of new spherical waves, the new front is the tangential surface of the secondary wave lets.'

The interaction of the incident wave with the boundary can be expended to cover the part of the disturbance that travels in to the second medium. (See Fig 4.)

$$AE = V_2t \qquad \text{---------- 2.2}$$

Comparing tri angle ABC and ABE shows that

$$AC = AB \sin \alpha, \quad \text{and} \quad AE = AB \sin \beta \qquad \text{---------- 2.3}$$

Where:- α is the angle of incidence which is the angle between the normal to the interface and the normal to the incident wave front .

β is the angle of refraction, which is the angle between the normal to the interface and the normal to the transmitted wave front.

$$\frac{BC}{AE} = \frac{ABSin\alpha}{ABSin\beta} = \frac{V1t}{V2t}$$

$$\frac{Sin\alpha}{Sin\beta} = \frac{V1}{V2} \qquad \text{---------- 2.4}$$

This equation is called the law of refraction for plane seismic wave often called **Snell's law** of refraction. However only one particular ray that is critically refracted wave from a boundary can be the source wavelet, which can be detected by the seismometer (geophones) at the surface of the earth. Since the angle of refraction of this case is 90°,equation (2.4) can be written as:-

$$\frac{Sin\alpha c}{Sin\beta} = \frac{Sin\alpha c}{Sin90} = Sin\alpha c = \frac{V1}{V2} \qquad \text{---------- 2.5}$$

Where: - α_c is the critical angle of incidence.

An individual particle vibrates back and forth as the seismic energy passes through the material in the direction of ray. However the displacement of the particle from its original position changes with time. This shows that many different paths lead the simple pulse of vibration from the source to a receiver. Because of the different distances and wave speeds along these various paths, pulses of vibration reach the receiver at different times .The effect of geometrical spreading; absorption, refraction and reflection are different along each of these paths. Therefore, the pulses of vibration will have different amplitude when they reach the receiver.

The same behavior of seismic wave transmission; at an interface is explained by Pierre de Fermat, (1601-1665) by the geometry of incident and seismic ray.

2.2.2 Fermat's principle

The passage of the seismic ray from a medium with velocity V_1 into a medium with higher velocity V_2 causes seismic ray refraction. In the figure below let A be a point on the incident ray at a vertical distance h from point C, and B be a point on the ray in the second medium at a distance h' from D (Fig.5).

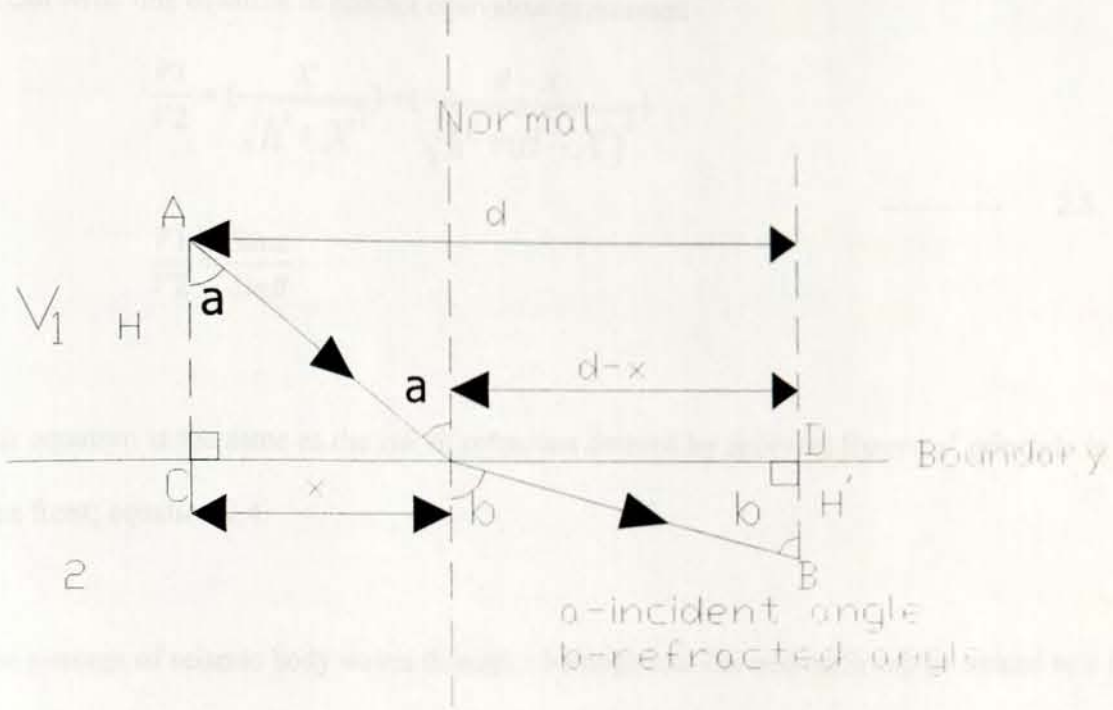

Fig.5. Seismic wave refraction at an interface

The distance CD is d, so that again OD is equal to (d-X). The travel-time t which have to minimize is given by: -

$$t = \frac{AD}{V1} + \frac{OB}{V2} = \frac{\sqrt{h^2 + X^2}}{V1} + \frac{\sqrt{h^2 + (d-X)^2}}{V2} \qquad \text{------- 2.6}$$

Differentiating the equation with respect to X and setting the result to zero for minimum **t;**

$$\frac{X}{V1\sqrt{h^2 + X^2}} - \frac{d-X}{V2\sqrt{h^2 + (d-X)^2}} = 0 \qquad \text{----------2.7}$$

We can write this equation in another equivalent expression

$$\frac{V1}{V2} = \left(\frac{X}{\sqrt{h^2 + X^2}}\right) \div \left(\frac{d - X}{\sqrt{h^2 + (d - X)^2}}\right)$$

---------- 2.8

$$\frac{V1}{V2} = \frac{Sin\alpha}{Sin\beta}$$

This equation is the same as the law of refraction derived by applying Hugyens' principle to the wave front; equation 2.4.

The passage of seismic body waves through a homogenous-layered earth can be treated to a first approximation in the same way. So that it is possible to use this vertical velocity structure for subdividing the Earth in to homogenous and isotropic layers, each with faster body -wave velocity than the layer above it.

2.3 GENERALIZED RECIPROCAL METHOD (GRM)

The GRM method (Palmer, 1980) is capable of mapping highly irregular refractors using the forward and reversed profile. GRM provides a graphical solution to resolve the geometry of sub-surface refractors. The principal difference of the GRM compared with the plus- minus and other time delay method is that the critically refracted rays emerge at or very near the same point on the refractor. GRM uses the offset (migration) distance refraction migration to obtain the detailed structure of a refractor about any localized lateral variation with in it. It is also able to resolve lateral variation in the refractor velocity. The method is especially important in engineering for

detecting weak zones, low rock strength and groundwater studies. It is also suited for computer implementation.

The horizontal separation between a point on the refractor where a ray is critically refracted and that at the surface The ray emerges from the same point of the refractor arrive at two different geophones locations separated by a distance X,Y. So that the GRM involves selecting several pairs of points (X, Y) and making a series of calculation to determine the optimum distance between them, $XY_{opt,}$ approximates the critical distance. The optimum distance is defined as the separation between a geophone in a forward-direction experiment and a geophone in the reverse-direction experiment such that the forward traveling and reverse traveling seismic rays emerge from a point on the refractor. Consequence of the geometry defined by the XY_{opt} is that the target refractor needs to be planar only over a very short distance in the vicinity of the point at which the two rays emerge from the refractor. To achieve maximum accuracy, the GRM requires knowledge of the critical distance.Determining this value is "potentially the most confusing aspect of the GRM"(Palmer, 1980:34). The XY_{opt} is relatively insensitive to dip however, accurate values are required if there are hidden zones.

The figure shown below (Fig.6) has three beds with the same strike but different dips θ_i. Depths Z_{Ai} and Z_{Bi} are measured normal to each interface a_i and b_i are down dip and up dip angles of incidence, respectively, and the angles at S and T are also critical angles .To get the travel time t_{AB} we consider a plane wave front PQ passing through A at time t=0;the wave arrives at C after traveling a distance

$Z_{A1} \cos a_1$, at time $t=(Z_{A1} \cos a_1)/V_1$

The wave front reaches R at the time;

$$t_{AR}=\sum_{1}^{2} (Z_{Ai}\cos a_i)/V_i \qquad \text{.....2.11}$$

The similar expression holds for t_{VB}. Because the wave is critically refracted at R and V, the time from R to V is RV/V_4. Generalizing, we get for n layers

$$t_{AB} = \sum_{1}^{n-1} (Z_{Ai}\cos a_i + Z_{Bi}\cos b_i)/V_i + RV/Vn \qquad \text{----------} \qquad 2.12$$

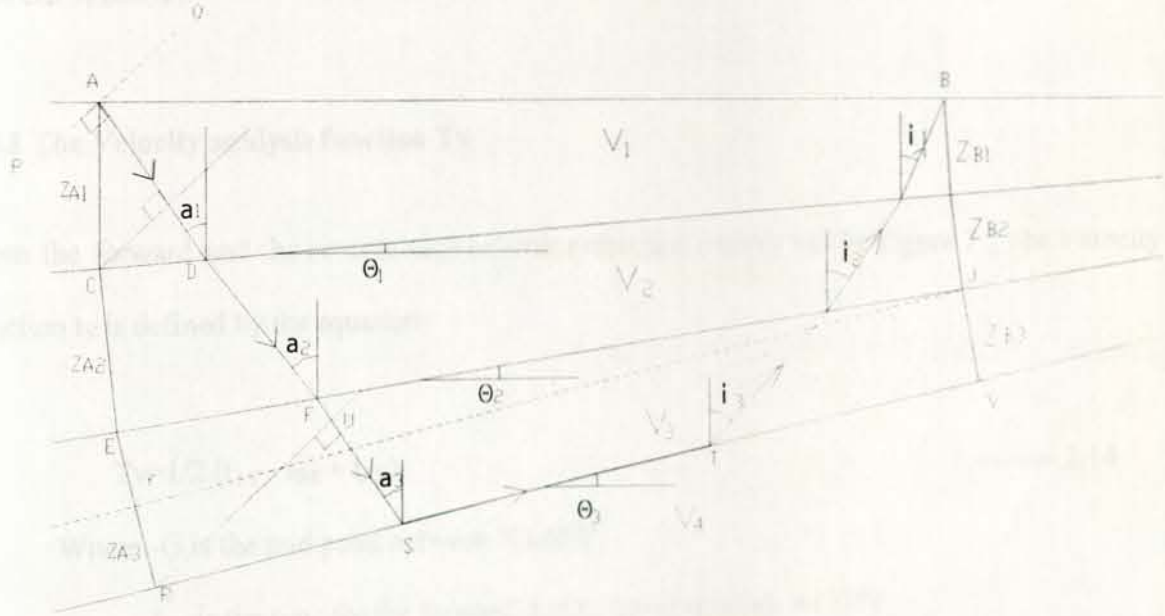

Fig.6. Ray path parameters for the four-layer earth model.(a= angle of incidence , I=angle of refraction ,θ= dip angle, Z_{Bi} =depth and V_i= velocity)

The distance RV=*YJ*=*EJ* Cos (θ2-θ1). In general we have

$$t_{AB} = \sum_{1}^{n-1} (Z_{Ai} \cos a_i + Z_{Bi} \cos b_i)/V_i + AB(Sn/Vn) \quad \text{----------2.13}$$

Where $Sn = \cos\theta_1 \cos(\theta_2-\theta_1).....\cos(\theta_{n-1}-\theta_{n-2})$.

We assume the dip increases slowly so that $\theta_i-\theta_{i-1} \cong 0$. In this case

$$Sn \cong \cos\theta_{n-1}$$

The generalized reciprocal method is based on the use of the computation of two functions. These are the velocity analysis function Tv and the time depth function T_G, referred to, the mid point between X and Y.

2.3.1 The Velocity analysis function Tv

From the forward and the reverse shot seismic refraction survey as the figure 7 , the velocity function t_V is defined by the equation:

$$Tv=1/2\ (t_{AY} - t_{BX} + t_{AB}) \quad \text{-------- 2.14}$$

Where:-G is the mid point between X and Y.

t_{AY} is the time for the forward shot to travel through ACG'Y.

t_{BX} is the time for the reverse shot to travel through BDG'X

t_{AB} is the time for the wave to travel through ACG'DB.

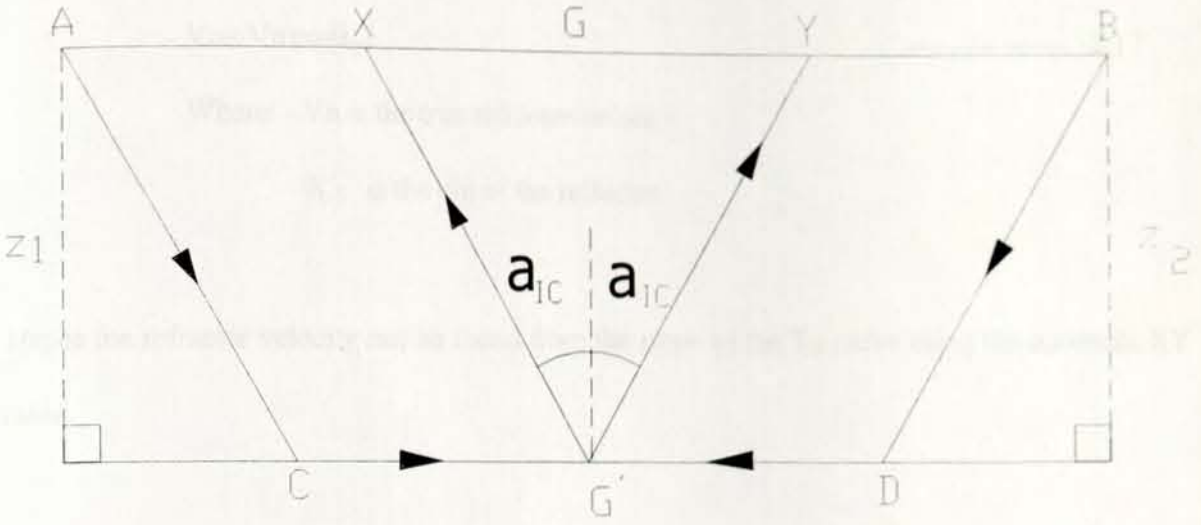

Fig.7 Ray path in GRM analysis(a_{ic} is the critical angle of refraction Z_i is depth)

The value T_V is calculated using this equation and plotted against distance for different XY values. The smoothest of this curve is the optimum value of XY in such away that both the reverse and the forward ray bounced from the same point of the refractor.

From trigonometric relationship and the wave equation the minimum distance (critical distance) between XY is given by:-

$$XY = Z_1 \tan a_{ic} + Z_2 \tan a_{ic} \qquad \text{---------- 2.15}$$

The inverse of an apparent refractor velocity Vn' is defined as the slope of a line fitted to the t_v values for the optimum XY. i.e

$$\frac{dTv}{dX} = \frac{1}{Vn} \qquad \text{---------- 2.16}$$

$$Vn \cong Vn'\cos\theta_{n-1} \qquad \text{---------- 2.17}$$

Where: - Vn is the true refractor velocity

θ_{n-1} is the dip of the refractor.

Hence the refractor velocity can be found from the slope of the T_V curve using the optimum XY value.

2.3.2. Time depth function T_G

The generalized time depth at G is defined by the equation:-

$$T_G = 1/2\ [t_{AY} + t_{BX} - (t_{AB} + XY/Vn')] \qquad \text{----------2.18}$$

Where: - Vn' the apparent velocity determined from the velocity function.

- Point A,B,Xand y are shown in fig.7 above.

If the dip is small $Z_{Xi} = Z_{Gi} = Z_{Yi}$. Thus T_G reduces to: -

$$T_G = 1/2\ [\sum_{1}^{n-1} Z_{Gi}(\cos\alpha_i + \cos\beta_i)/V_i\ ] \qquad \text{----------2.19}$$

From equation (2.19); the expression $2\ V_i/(\cos\alpha_i + \cos\beta_i)$ is defined as depth conversion factor(D.C.F)

This implies,

$$\sum_{1}^{n-1} Z_{Gi} = T_G \times (D.C.F) \qquad \text{----------2.20}$$

Assuming horizontal plane layers, therefore equation (2.19) becomes

$$T_G = 1/2 \left[\sum_{1}^{n-1} Z_{Gi}(\cos\alpha_I)/ V_i \right. \qquad \text{----------2.21}$$

And using Snell'law $\sin\alpha_i = Vi'/ Vn'$;If we replace the actual section by a single layer of thickness, $Z_T = \Sigma Z_{Gi}$ and constant velocity V with an angle of incidence a such that

$$T_G = (Z_T \cos\alpha)/V \ ; \ \sin\alpha = V/ Vn' \qquad \text{----------2.22}$$

For a horizontal layer cases; Equ (2.15) can be expressed as:-

$$XY_{opt} = 2\sum_{I=1}^{N-1} Z_{Gi} \tan\alpha i \qquad \text{----------2.23}$$

When we write this by a single constant velocity;

$$XY = 2Z_T \tan\alpha i \qquad \text{----------2.24}$$

Eliminating Z_T and α between equ. (2.21) and equ. (2.24) ,then

$$V = \{Vn'[XY/(XY + 2 T_G Vn')]\}^{1/2} \qquad \text{----------2.25}$$

It is an expression of the average velocity for multi layer lithological units. Similarly the thickness of these beds can be calculated by slight modification of equ (2.21) above as;

$$\sum_{1}^{n-1} Z_{Gi} = T_G \bar{V} / \cos \bar{i} \qquad \text{----------2.26}$$

Where :- $\cos \bar{i} = \sin^{-1}(\bar{V} / V_n)$

Hidden zones (because of thin layers) and velocity inversion are the most common source of errors in the majority of refraction methods (Palmer, loc.cit: 39). When data are good it is possible to defined both problems by comparison of the XY_{opt} from the most detail T_G curve and the most simplest T_v curve with the calculated XY_{opt} using equ(2.24).

When the calculated XY_{opt} is greater than the observed $XY_{opt;}$ it is an indication of hidden layer and as a result the real depth of the refractor is less than the calculated one using equ(2.26). Where as when there is thin layer the calculated XY_{opt} is less than the observed XY_{opt} so that the real depth of the refractor is greater than the calculated one.

CHAPTER-3

FIELD PROCEDURE AND DATA ACQUISITION

Controlled source seismology involves the detonation of seismic explosive charge in deep bore holes distributed along profiles of seismic recording instruments that are deployed at regular interval on the earth surface. All logistics arrangement of the fieldwork as acquisition of explosives, drilling the necessary bore holes as well as obtaining permissions to undertake the seismic shots were arranged by the EAGLE group. The EAGLE project designed to carryout two seismic profiles;the first,profile 1,across the Ethiopian rift in the vicinity of Nazrate extending to the Blue Nile in the northwest and to Ginir(inBale region) in the southeast; the second profile2,extended along the rift from Awassa in the south to Gewane in the north. In this study the part of EAGLE across rift profile is taken in to consideration to understand the subsurface structure of upper crust across the Main Ethiopian Rift.

From the total of 19 shots fired by EAGLE project only 5 shots are considered for this study. These selected borehole EAGLE shotpoints (SP) found at Derba (SP13), ChefeDonsa (SP14), Doni B (SP25), Kula (SP16) and Bele (SP17). The holes were drilled using an air rotary system through the overburden and then down the hole hammer (DTH) to the bottom with a minimum depth of 50m and diameter of 10'.

The seismic explosive charge type used on the work was powergel C+ with primex booster and explosive cords. The charge size loaded at each hole on average was 1 tone.

SHOT HOLE DATA

Table-1 Shot holes location and depth

No	Site name	identification no.	Location			Elvation (m)	Depth (m)	Ground Level (m)
			Easting	Northing	Zone			
1	Derba	SP13	464199	1034792	37	2458	50	24.15
2	Chefe Donsa	SP14	513296	992641	37	2368	50	Nil
3	Doni B	SP25	568063	943141	37	1236	70	11
4	Kula	SP16	575823	886441	37	2502	50	33.4
5	Bele	SP17	613831	854223	37	2415	50	40.45

Table-2 Shot time and charge size

No	Site name	identification no.	Shot Date	Shot Time (GMT)	Timer used	Explosive size (kg)
1	Derba	SP13	13 Jan/03	21:20:05	uphole	600
2	Chefe Donsa	SP14	12 Jan/03	21:03:00	GPS/Leics	375
3	Doni B	SP25	12 Jan/03	21:50:00	El paso	1025
4	Kula	SP16	13 Jan/03	21:10:00	USGS	1100
5	Bele	SP17	12Jan/03	21:10;00	USGS	2500

The maps shown below show the shot point location and the profile line of the study area.

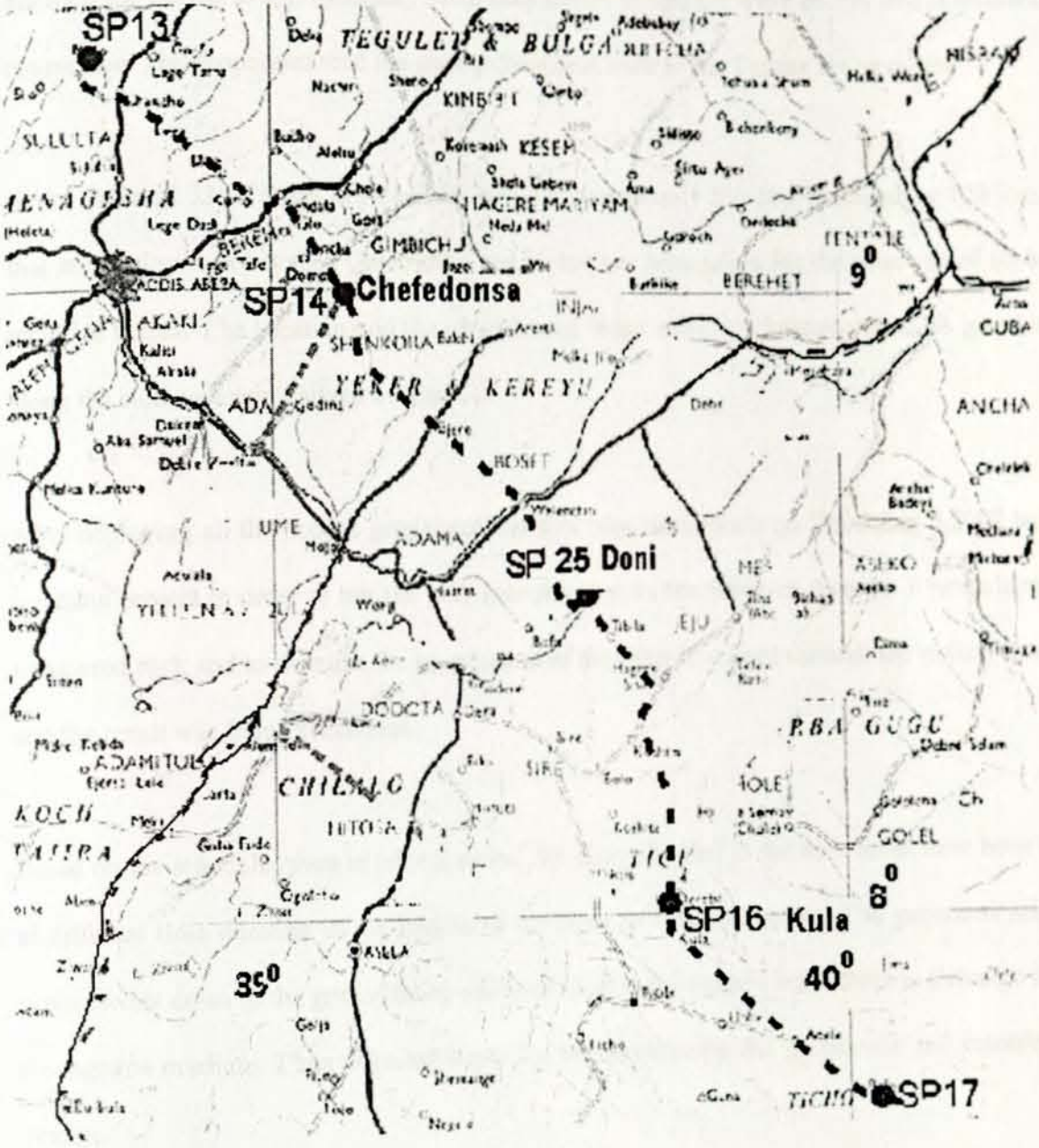

Fig.8. Map showing the shot points and Texan profile

(Map modified from EAGLE phase III profile)

The instrumentation on the EAGLE project included two different types of seismic recorder; Gurlap broadband systems (6TD) and Reftex Texan (being a 1-channel recorder with a single

vertical 4.5 Hz geophone). The series of geophones deployed at a normal spacing of 1 km. distance and buried in approximately 15cm deep trench picked the wave energy that is returned to the surface. The geophones send the wave information back to the Texans for recording.

From the total 339 Texans deployed for EAGLE project only the data recorded by 120 Texans that are deployed in between Chefedonsa and Kula have been taken for the selection of 68 best-recorded traces. The location and the elevation of those relatively best-recorded 68 geophones along the study are summarized in annex-D.

After deploying all the needed geophones test shot was taken place on December 5,2002 before the main project in order to test the bore hole response to the firing on average 1 tone charge in weathered rock and to examine the propagation of the seismic energy through the tertiary basalts, and the result was found successful.

Based on the schedule given in table 2 above, the charge loaded in the bore holes have been fired at different time duration in the middle of the night to minimize noise. The generated seismic wave travels down to the ground being refracted back to the surface when there is a change in the propagation medium. Thus refracted wave has been sensed by the geophones and recorded by Texans.

The Seismic trace recorded by the Texans has been prepared for first arrival picking using the seiswide soft ware and the resulting trace and the pick is shown below.

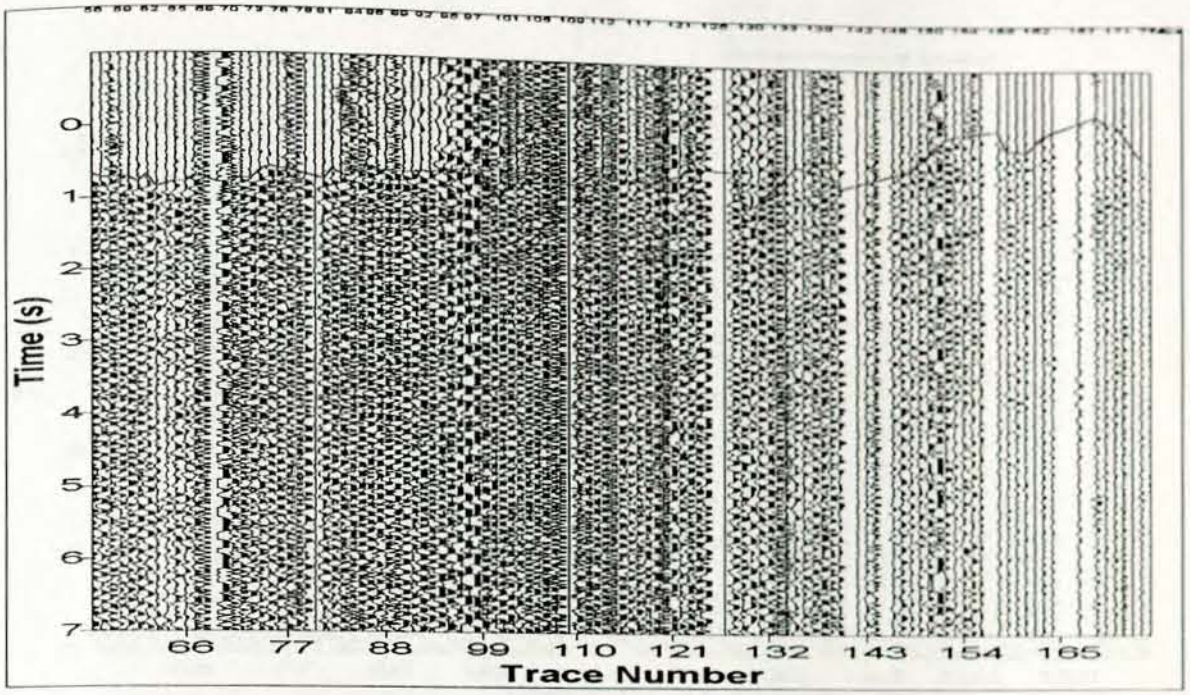

Fig.9 Seismic record from shot-13 and the first arrival pick

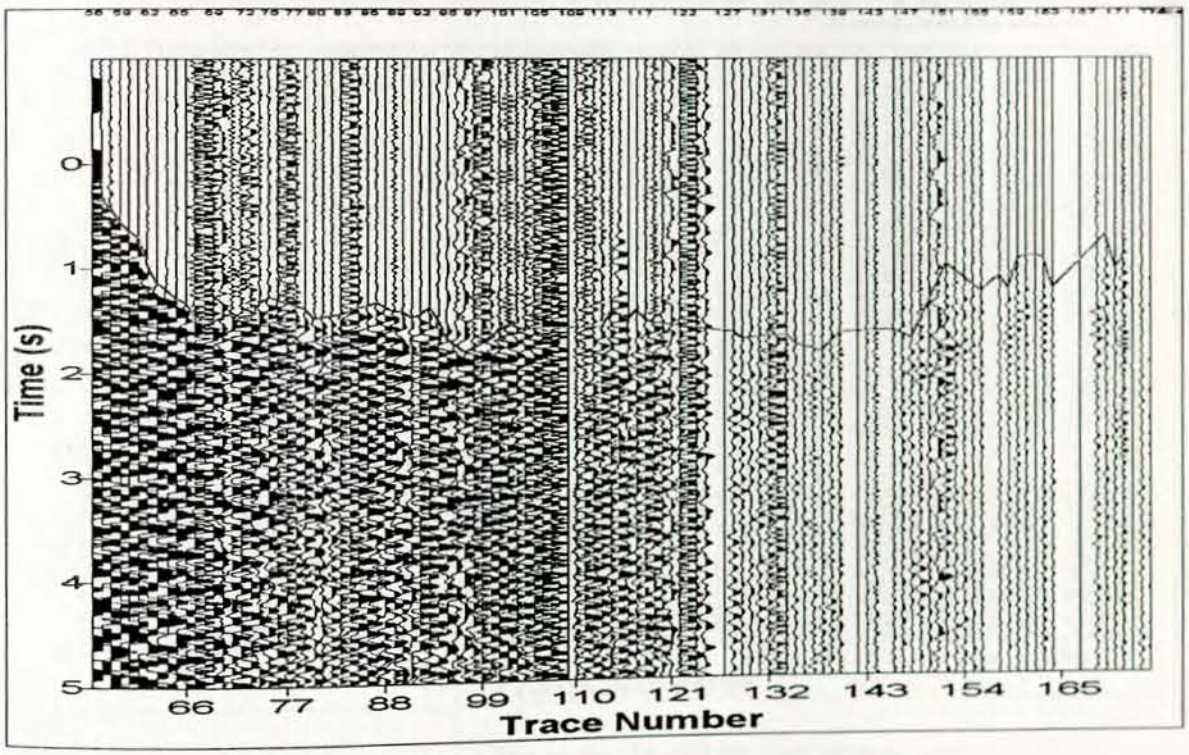

Fig.10 Seismic record from shot-14 and the first arrival picks

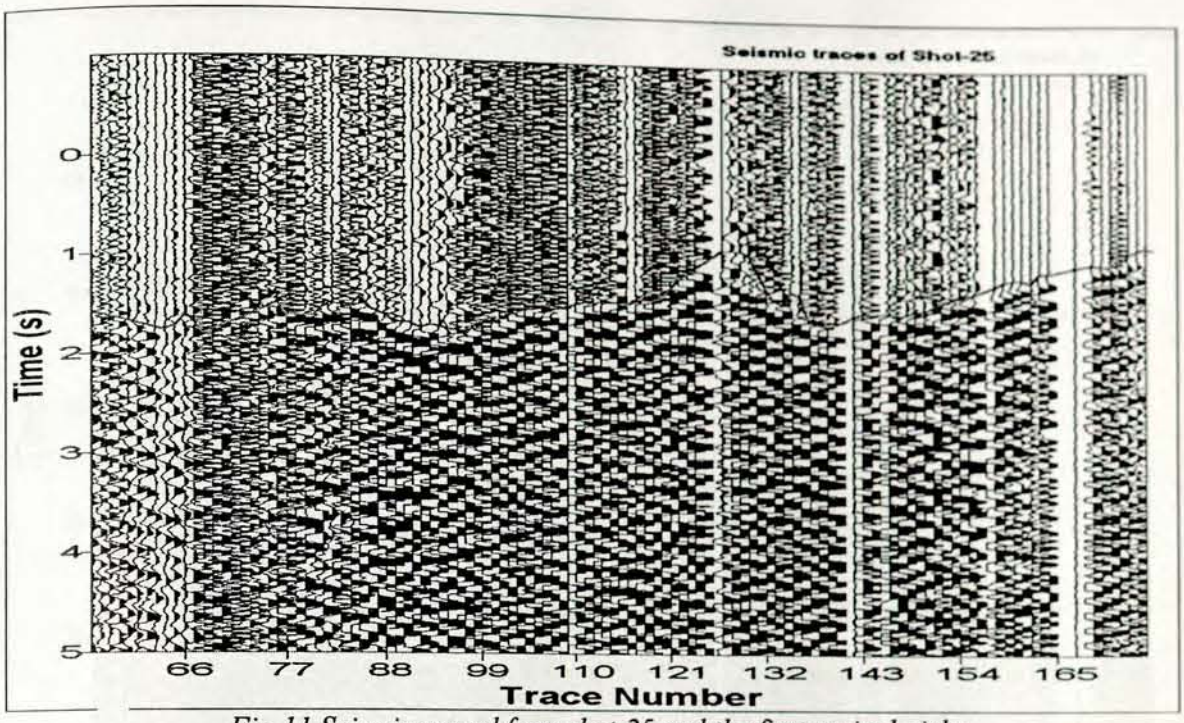

Fig.11 Seismic record from shot-25 and the first arrival picks

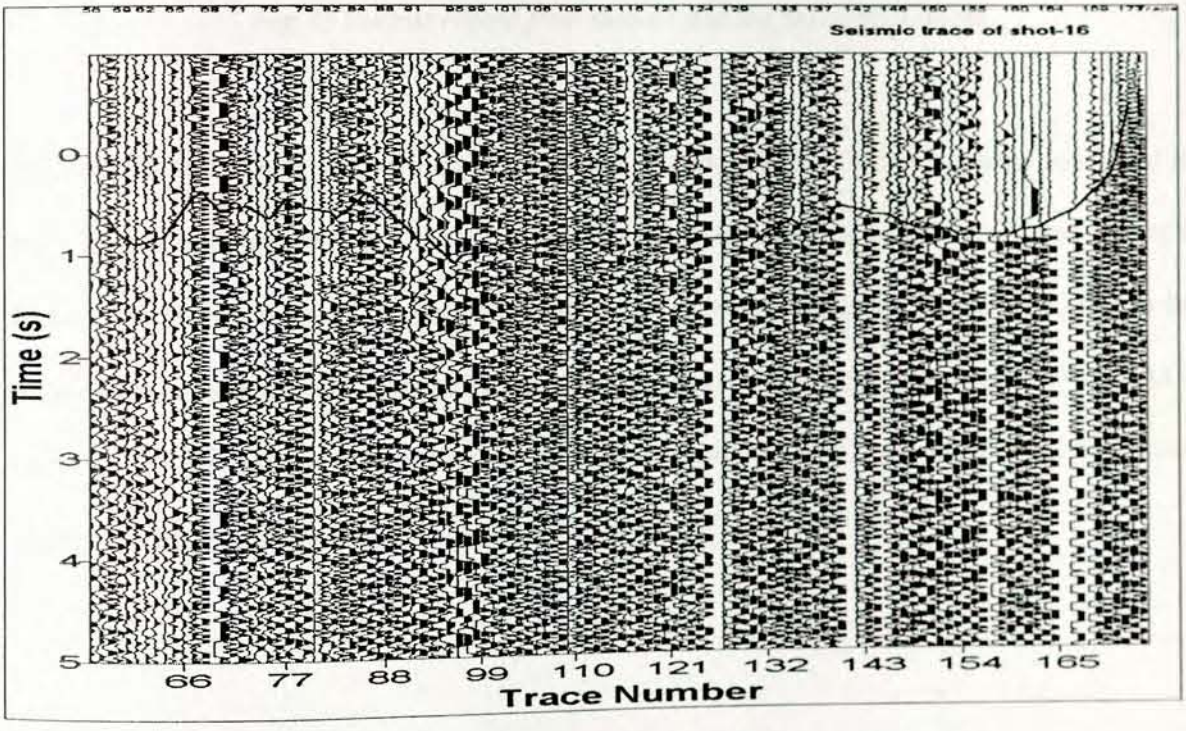

Fig.12 Seismic record from shot-16 and the first arrival picks

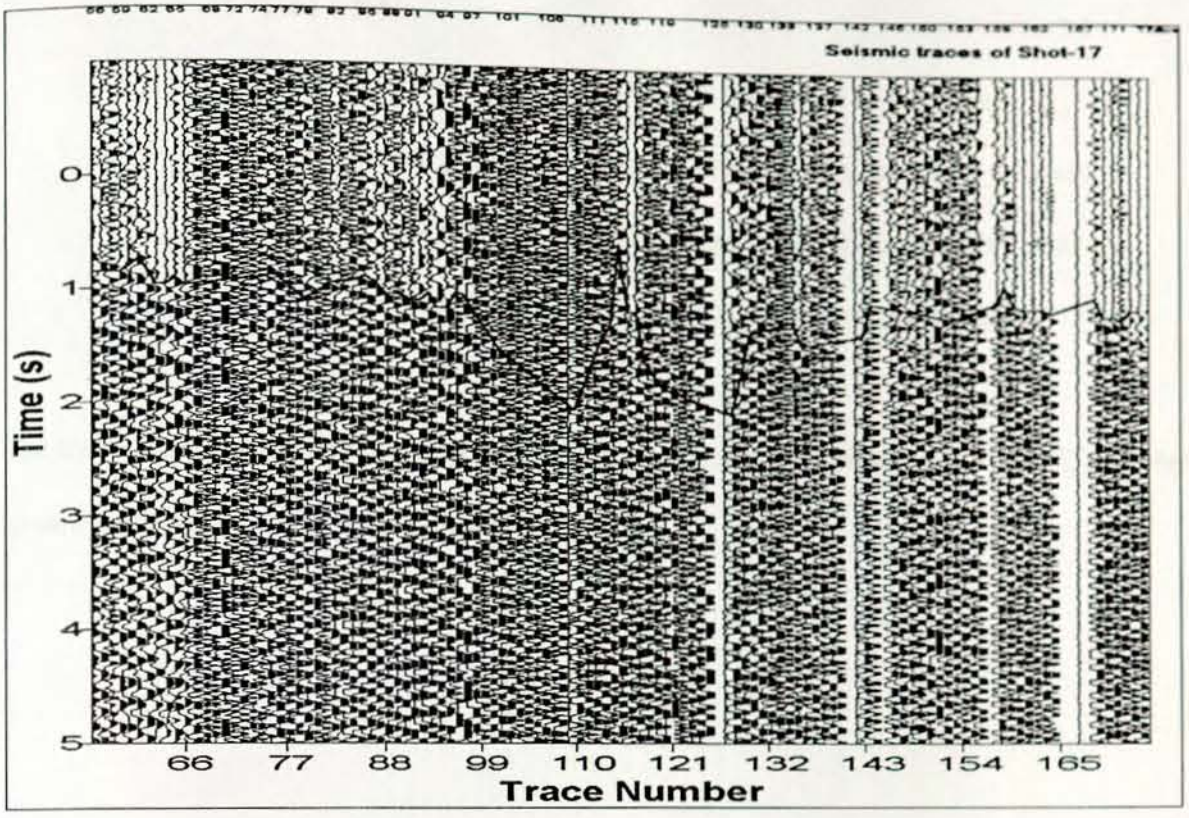

Fig.13 Seismic record from shot-17 and the first arrival picks

The seismic signal received by the geophones and recorded by the Texans has been converted in segY format and prepared for first arrival picking using the seiswide soft ware .To use the segY format, the arrival time of the Head wave (the first arrived wave to each geophone) has to be reduced by considering the average velocity of seismic wave in upper mantle (=6000m/s). As a result of this the reduced time that are directly picked from the seismic trace (Fig 9-13) have been changed to the normal arrival time based on the following equation.

$$Tt = Tred + X/V \qquad \text{----------3.1}$$

Where:- Tt is the arrival time of the head wave in given trace

Tred is the reduced arrival time as it is picked from the trace

X is offset distance of each geophone from the active shot.

V is average velocity of seismic wave in upper mantle.

The travel time of each wave trace from the five shots has been calculated (see Annex-D) inorder to analyze these data using GREMIX software.

DATA PROCESSING

The software type to analysis and interpretation of the collected seismic data is GREMIX. GREMIX software is a special designed package to assist in the interpretation of seismic refraction data interms of laterally varying layered earth structure with the features of the generalized reciprocal method (Palmer, 1980).

At the initial the five shots selected and labeled based up on the GRM shot labeling convention.

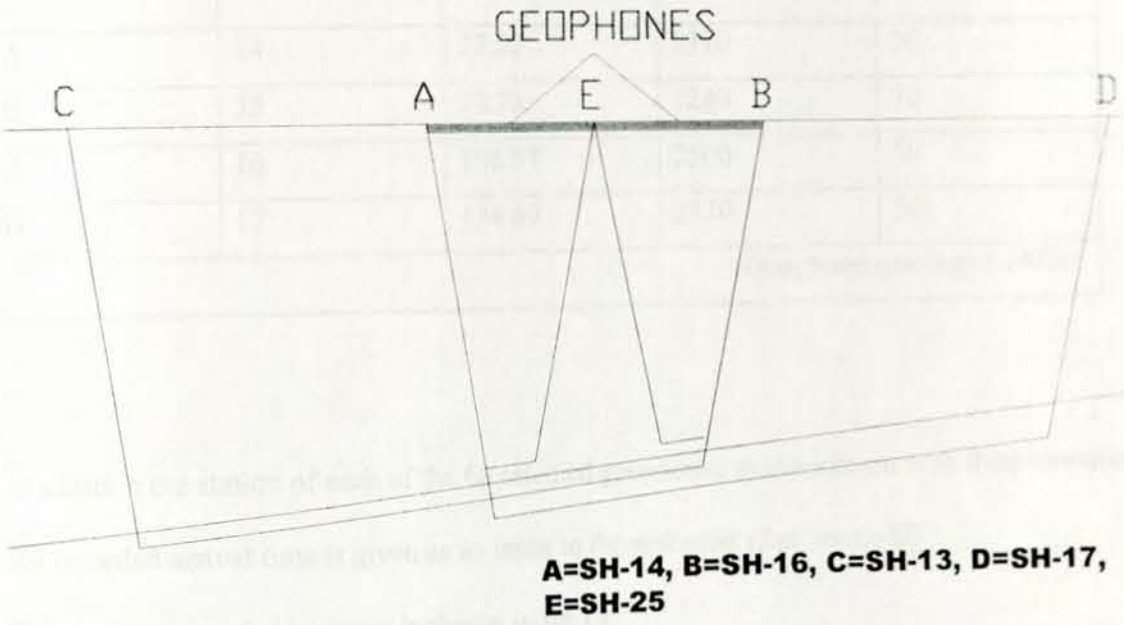

Fig.14 The Shot–Geophone arrangement used in the analysis.

Shot-13 and Sh-17 are far end shots; Shot-14 and Sh-16 are end shots while Sh-25 is the interior shot. The Geophones were deployed in between the end shots as it is shown in the figure (Fig. 14)

4.1 DATA ENTRY

Gremix required the exact position of each geophone and shot based up on the nomenclature shown in Figure14. And this position has to be entered interms of station, rather than the actual distance. By taking the offset of other shot points from shot –13 (see table-3), the data shown in table below is fed in to the software.

Table 3: -The station of the shots starting from Sh-13

Type	Shot No.	Station (Km)	Elevation (m)	Depth (m)
C	13	0	2400	50
A	14	37.07	2370	50
E	25	79.73	1240	70
B	16	106.57	2500	50
D	17	134.60	2420	50
				Geophone spacing=1.74Km.

In addition the station of each of the 68 selected geophones in association with their elevation and the recorded arrival time is given as an input to the software. (See annex-D)

The resulting travel time curve is shown in fig.15.

4.2. ASSIGN ARRIVALS TO LAYERS

Layer assignments used to determine the velocity and the depth of each refractor. The full screen assignments of arrival to layers are shown (See fig15). After assigning layers arrival time the pair shots would be selected by observing the number of over lap points for Phantoming.

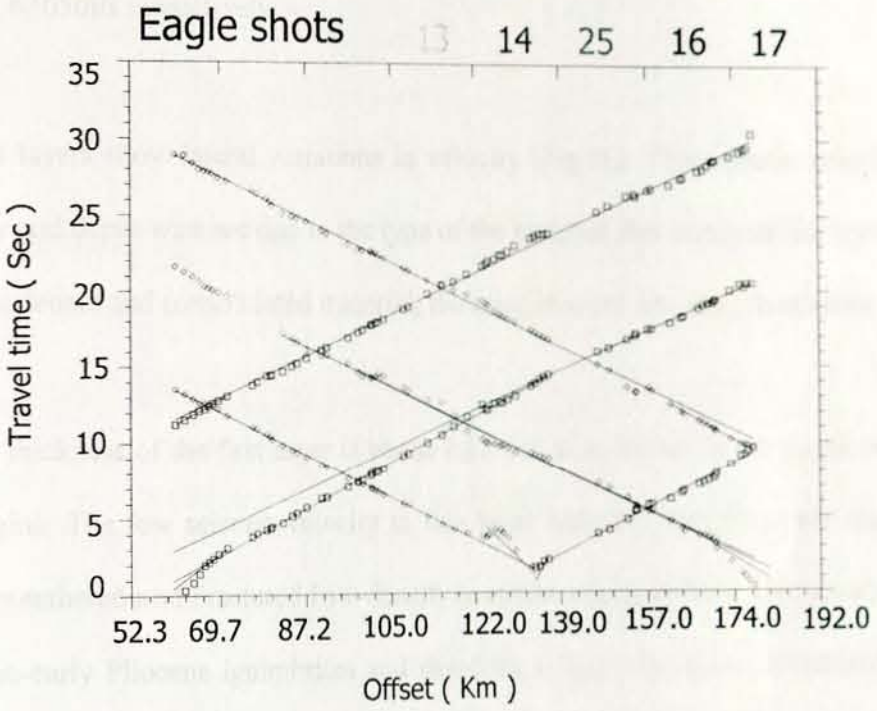

Fig.15. Travel time curves and layer assignment.

From the time depth section of the pair shots, from the seven different X-Y value, the most detailed one will be taken and this choice of X-Y value would be checked by the X-Y value found from the smoothest curve of velocity analysis curves. Finally when the time section is displayed, editing was done inorder to remove conflict layer boundaries.

CHAPTER-5

RESULTS AND INTERPRETATION

The results of the study reveal that there are four major seismic layers across the Main Ethiopian Rift. The average seismic velocities of the layers from top to bottom are 3 000 m /s, 4 500m/s, 5560m/s and 6365m/s respectively.

However the layers show lateral variations in velocity (Fig.16). This seismic velocity variation both laterally and depth wise are due to the type of the material that comprise the layer. When the layer consists denser and consolidated material, the seismic wave shows high velocity.

The average thickness of the first layer is about 2.17 km. It is thinner at the center comparing to the rift margins. The low seismic velocity in this layer indicates that the upper crust has been covered by weathered and fractured low-density material which include Quaternary sediments, Late Miocene-early Pliocene ignimbrites and rhyolites, Oligocene basalts, Mesozoic sediments, etc. This layer has relatively low velocity in the center of the model, which is the floor of the Main Ethiopian Rift. The decrease in velocity endorsed with the series of faults and fractures of the area due to the tectonic activity in the region.

The average thickness of the second layer is 3Km. It is rugged refractor and its velocity uniformly increases from the western margin to the eastern margin. The seismic velocity through this layer is relatively lower than the underlying layers (4500m/s). This could probably represent

Fig.16. GEO-SEISMIC MODEL ACROSS THE MAIN ETHIOPIAN RIFT.

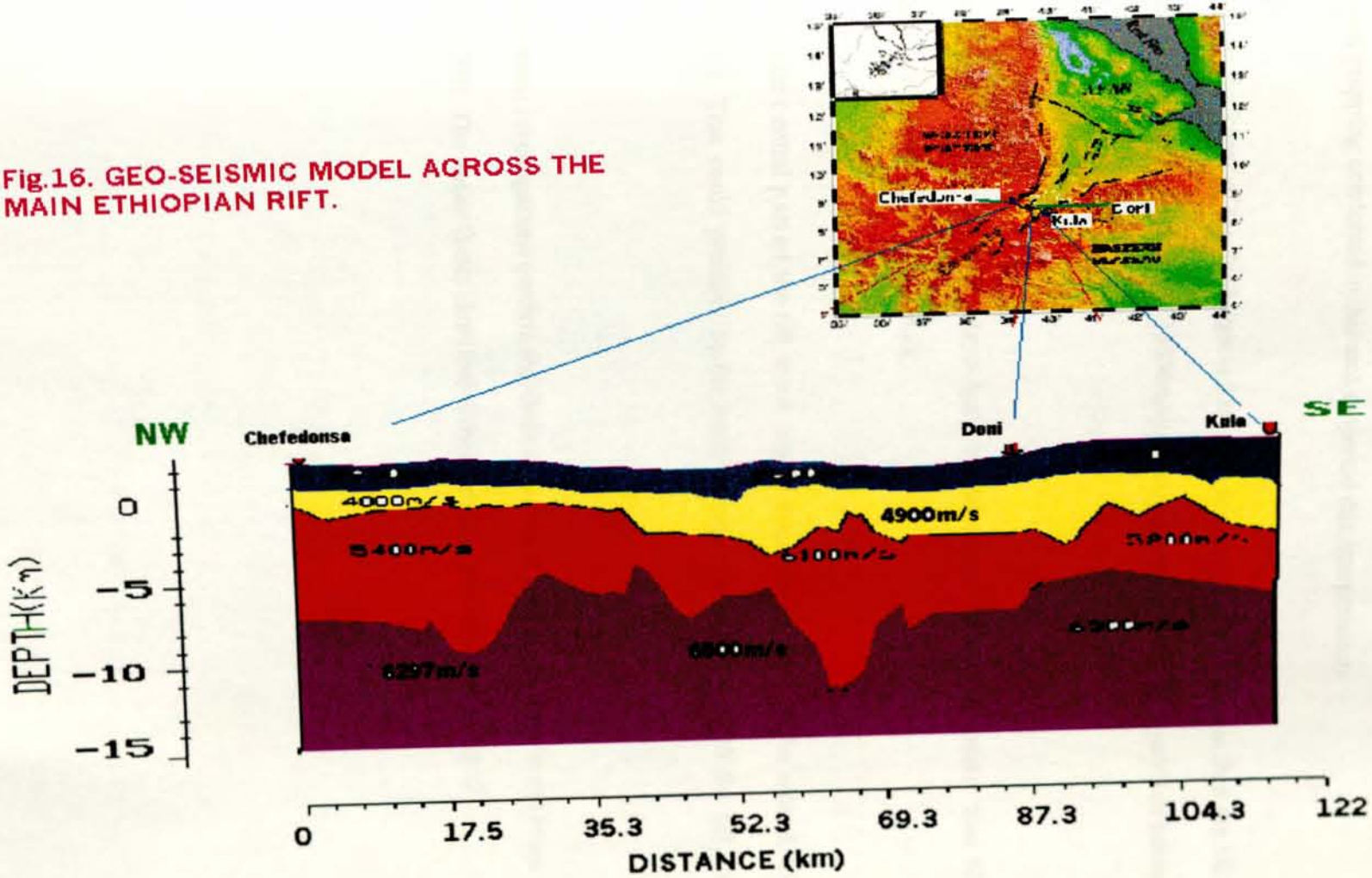

the series of metasediments and metavolcanics of the low-grade metamorphic basement. Geological mapping conducted in that area supported this interpretation.

The average thickness of the third layer is 5 km. It is thicker in the NW margin than the SE. The seismic velocity in this layer is high (5300m/s) and this corresponds to the crystalline basement rock.

The seismic velocity in the fourth layer has a typical crustal velocity of greater than 6300m/s. This probably is maffic, ultramafic rock.

Generally the central part of the rift shows higher velocities (Fig.16) in the second, third and fourth layers. This could probably be the result of mafic intrusions beneath the rift magmatic centers.

The geological investigations confirm that there are series of fault alignments in the Main Ethiopian Rift. The major faults identified in the study area are indicated in Fig.17.

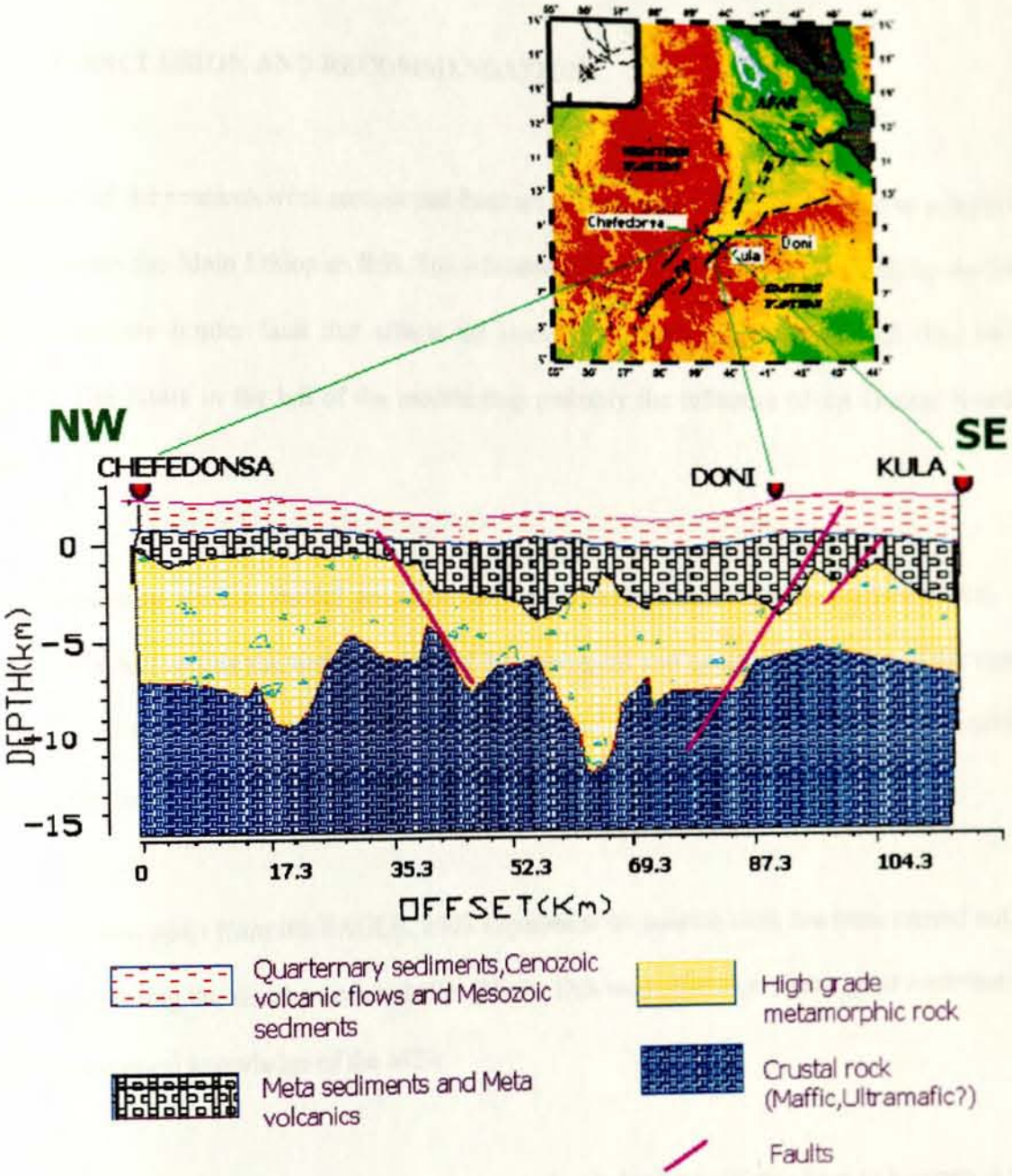

Fig 17. The inferred Geological section beneath the Main Ethiopian Rift

CHAPTER 6

CONCLUSION AND RECOMMENDATION

The result of the research work reveals that there are four major seismic layers down to a depth of 10 km across the Main Ethiopian Rift. The rift-eastern plateau margin is clearly seen by the NE-SW Assela-Sire border fault that affects the layers by dragging them downwards (Fig 16 & Fig.17). The faults in the left of the models may probably the influence of the Gurage boarder fault.

The preliminary seismic model produced from the result of this research work will play an important role towards the understanding of the geological and geophysical nature of the upper most part of the crust beneath the Main Ethiopian Rift. This result surely serves as a starting material for future more detailed study of the Ethiopian Rift subsurface.

It is noted that apart from the EAGLE, 2003 experiment no seismic work has been carried out in the past regarding the structure of the MER (2003). This work, therefore, has a great contribution to the geophysical knowledge of the MER.

Since the MER is a very active tectonic area, more detailed seismic studies have to be done in the future inorder to understand the geological and geophysical situation for producing more refined Geoseismic model. The detailed seismic studies may help to know the geological structures as well as the geological processes activate in the rift. Based on the results obtained from such

studies closely related seismic risk assessment can also be undertaken that will greatly benefit the growing towns in the rift valley.

For further investigation of subsurface material to the depth of upper mantle the whole seismic data of the EAGLE cross rift profile have to be analyzed as a single spread. Inaddition to identify the Cenozoic volcanic flows and the Mesozoic units including the low velocity layers of the upper most crust, other geophysical methods like Gravity method and seismic reflection are recommended.

The central part of the model that is the floor of the Main Ethiopian Rift shows a relatively low velocity in the first layer while high velocity in the second third and fourth layer. Additionally the refractors have highly undulated topography. This may be due to the tectonic activity and the magmatic process underneath; therefore detail Gravity and Electrical resistivty survey has been recommended to know the heat anomaly of the area due to the observed situation. The result will play a great role for employment of the geothermal energy source that may contributes a lot for the economic development of the country.

REFERENCES:-

-Alemu, A., 1992,the Gravity Field and Crustal Structure of the Main Ethiopian Rift,Ph.D Thesis,Stochholm

-Assfaw, L.M., 1986, Catalogue of Ethiopia earthquake parameters, strain release and seismic risk, Geological survey of Ethiopia

-Berckhemer,H., 1975,Deep seismic sounding in the Afar region and the high lands of Ethiopia,A.pilger,Stuttgart.

-Di Paola, G.M.,1972. The Ethiopian Rift Valley. Bull

-Dobrin, M.B, 1976, Introduction to geophysical prospecting: McGraw-Hill Book Company New York.

-Ethiopia Afar Geoscientfic Lithospheric Experment, 2003,Unpublished report.

-Ewing, W.M., and Heezen, B.C., 1956. Some problems of Antarctic Geology,Monogr

-Gass, I.G., 1970 a,b., The evolution of volcanism in the southern area of the Red sea, Gulf of Aden and Ethiopian rifts. Philos,Trans.R.Soc,England

- Gibson, I., 1968, The structure of volcanic Geology of An axial portion of the Main Ethiopian Roft, Amsterdam

-Kazmin,V. and Berhe,S.,1978. Geology and development of the Nazret area. Ethiopian institute of Geological Survey

- Korme, T., 1997, Volcanic vents rooted on extension fracture and their Geodynamic implications in the Ethiopian Rift, Journal, Paris.

-Lloyd,E.F.,1977.Geological Factors Influencing Geothermal exploration in the Langano region,Ethiopia,Report

-Lowrie W., 1939,Fundamental of geophysics, Cambridge, New York.

-Luleseged Ayalew, 1990,Engineering geological characteristics of the clay soil of the Bole area, their distribution and practical importance (M.sc.thesis), AAU.

-Mathewson, C.C., 1981,Engineering geology, Charles E.Merill publishing company, Columbus.

-McConnel, R.b.,1967. The East African Rift system, Nature, Addis Ababa

-Milsom,J., Field Geophysics,Geological Society of London,England

-Mohr,P.,1960.Report on Geologica Excursion trough Southern Ethiopia,Bull Geophy,Obs.Addis Ababa.

- Mohr.P, 1962b.The Ethiopian Rift System.BullGeophys.Obs.,Addis Ababa.

-Mohr.P, 1966b.Geological report on the Lake Langano and adjacent plateau regions. Bull Geophy,Obs.Addi Ababa

-Mohr.P, 1967, The Ethiopian Rift system. Bull Geophysical observatory, Addis Ababa

-Morton et.al.,1979,Geological Map of Addis Ababa, Unpublished

-Tefera M., 1996, Ethiopian geological Map, Ethiopia Geological survey, Addis Ababa

.

-Palmer,D. ,1980,The Generalized Reciprocal Method of seismic refraction interpretation: Tulsa,Oklahama,Socity of Exploration Geophysics.

-Reynolds.M.J.,1997, An introduction to applied and environmental Geophysics, Geo-scie Ltd,UK.

-Robinson,E.S.,& Coruch, 1988,Basic exploration geophysics, John Wiley &Sons, N.Y

- Rosendahl,B.,1986.Stractural expressions of rifting, Geological Society Publication

-Solomon Yohannes, 1982,Case studies of building damage to expansive soils in Addis Ababa (M. Sc. Thesis), AAU.

-Telford W.M., Gildart L.P., Sheriff R.E., and KeysD.A.1978, Applied geophysics, Cambridge university press, England

-W.Lankston, R., 1990.The seismic refraction method: a viable tool for mapping shallow target into the 1990s

-Wolde,B.,1989.Cenozoic Volcanism and Rift development in Ethiopia, Addis Ababa university, Ethiopia.

ANNEXS

Annex-A. P-wave velocities of some materials

Geological material	Vp (m/s)
Water	1450-1530
Petroleum	1300-1400
Loess	300-600
Soil	100-500
Snow	350-3000
Solid glacier ice	3000-4000
Sand loose	200-2000
Sand (dry, loose)	200-1000
Sand (water saturated loose)	1500-2000
Glacial moraine	1500-2700
Sand and gravel (near surface)	400-2300
Sand and gravel at 2 km depth	3000-3500
Clay	1000-2500
Estuarine muds/ clay	300-1800
Flood plain alluvium	1800-2200
Permafrost quaternary sediments	1500-4900
Limestone (soft)	1400-4500
Limestone (hard)	2800-7000
Dolomites	2500-6500
Anhydrite	3500-5500
Rock salt	4000-5500
Gypsum	2000-3500
Shale	2000-4100
Granites	4600-5200
Basalts	5500-7000
Peridotite	7800-8400
Serpentinite	5500-6500
Gneiss	3500-7600
Marbles	3780-7000
Sulphide ores	3950-6700
Pulverised fuel ash	600-1000
Made ground (rubble etc.)	160-600
Landfill refuse	400- 750
Concrete	3000-3500
Disturbed soil	180-335
Clay land fill cap (compacted)	355-380

Annex-B. Geophones locations in the study area

Geophones Location							OFFSET(Km)
order	trace	site	easting	northing	zone	ELVA(m)	From SH-13
1	56	1156	513618	992341.1	37P	2381	65.189
2	57	1158	515238.4	991417	37P	2329	67.019
3	58	1159	515965.4	990963.9	37P	2318	67.867
4	59	1160	516172.4	989946.4	37P	2301	68.688
5	60	1161	515947.7	988799.7	37P	2296	69.278
6	61	1162	515975.3	987856.2	37P	2275	69.926
7	62	1164	515819.1	986086.3	37P	2280	71.016
8	63	1165	515985.5	985126.1	37P	2233	71.799
9	64	1166	516365.5	984373.3	37P	2190	72.599
10	65	1167	516539.3	982974.1	37P	2168	73.696
11	66	1169	517658.2	981629.3	37P	2169	75.442
12	67	1172	526598.8	983826.8	37P	2362	80.616
13	68	1173	527102.8	982871.8	37P	2362	81.614
14	69	1174	527495.9	981855.4	37P	2367	82.569
15	70	1175	528467.4	981602.5	37P	2452	83.475
16	71	1176	528928.8	980822.3	37P	2474	84.33
17	72	1177	528221.4	979705.7	37P	2414	84.516
18	73	1178	527426.2	978620.8	37P	2403	84.626
19	74	1180	527173.8	976560.6	37P	2390	85.824
20	75	1181	527807.9	975782.8	37P	2375	86.822
21	76	1183	528594.4	973848.7	37P	2316	88.717
22	77	1184	529081.8	972955.4	37P	2288	89.684
23	78	1185	529080.5	971828	37P	2267	90.609
24	79	1186	530165.4	971330.3	37P	2274	91.597
25	80	1187	530439.5	970316.4	37P	2251	92.501
26	81	1188	530238.2	969303.5	37P	2252	93.062
27	82	1190	530772	967620.1	37P	2182	94.637
28	83	1191	531718	967126.7	37P	2147	95.654
29	84	1192	534384.9	966580.4	37P	1820	97.936
30	85	1193	535388.5	966024.6	37P	1766	99.044
31	86	1194	536013.6	965172.1	37P	1740	100.089
32	87	1196	537177.2	963361.4	37P	1691	102.19

			Geophones Location				OFFSET(Km)
order	trace	site	easting	northing	zone	ELVA(m)	From SH-13
33	88	1197	537694.4	962570.6	37P	1672	103.114
34	89	1199	539636.9	962205.8	37P	1654	104.758
35	90	1200	540588.5	962779	37P	1653	105.055
36	91	1201	541614.9	962853	37P	1631	105.75201
37	92	1202	542476.8	962990.6	37P	1591	106.29001
38	93	1203	543228.4	962209.4	37P	1565	107.37801
39	94	1205	544569.8	960694.2	37P	1520	109.38601
40	95	1206	545233.8	959817.8	37P	1503	110.47501
41	96	1207	545957	958983.8	37P	1486	111.56801
42	97	1208	546642	958238.9	37P	1475	112.58401
43	98	1210	546500.4	955531.9	37P	1463	114.33501
44	99	1211	546637.1	954164.4	37P	1468	115.39301
45	100	1212	547551.7	953312.2	37P	1523	116.64201
46	101	1213	548437	952892.1	37P	1599	117.56601
47	102	1215	550008.8	952139.3	37P	1662	119.22201
48	103	1216	549709	951208.7	37P	1709	119.65801
49	104	1217	550009.3	950104.4	37P	1824	120.64601
50	105	1218	550722.1	949358.2	37P	1850	121.67101
51	106	1220	549552.5	947504.9	37P	1892	122.16501
52	107	1221	549863.3	946586.7	37P	1986	123.03901
53	108	1222	550417.4	945950.8	37P	2018	123.87901
54	109	1223	551128.1	945307.6	37P	2060	124.84001
55	110	1224	552055.9	944363.3	37P	1940	126.16301
56	111	1225	552526	943591.1	37P	1869	127.04801
57	112	1227	552153.9	941967.5	37P	1761	127.96401
58	113	1228	552288.8	941056.4	37P	1714	128.71901
59	114	1229	551817.3	940051.4	37P	1610	129.13201
60	115	1230	551286.1	939201.2	37P	1517	129.40201
61	116	1232	550594.3	937150.7	37P	1455	130.46701
62	117	1233	551029.6	936020.7	37P	1454	131.60101
63	118	1234	552033.8	936189.7	37P	1458	132.13701
64	119	1236	553998.4	936559.6	37P	1430	133.18301
65	120	1237	554978.5	937084.2	37P	1428	133.46101
66	121	1239	556855.6	937515.8	37P	1393	134.42901

			Geophones Location				OFFSET(Km)
order	trace	site	easting	northing	zone	ELVA(m)	From SH-13
67	122	1240	557656.6	937962.6	37P	1357	134.66301
68	123	1241	558614.9	938640.3	37P	1321	134.84401
69	124	1243	560287.3	939475.3	37P	1283	135.43101
70	125	1244	560485.6	940401.7	37P	1295	134.92901
71	126	1245	561830.9	940585.7	37P	1266	135.76301
72	127	1247	563334.5	938908.2	37P	1269	138.008
73	128	1248	563637	938057.5	37P	1281	138.823
74	129	1249	564053.9	937125.7	37P	1295	139.76701
75	130	1250	564439.4	936347.4	37P	1300	140.58801
76	131	1251	564889.0	935518.1	37P	1312	141.49201
77	132	1253	566050.7	934159.3	37P	1339	143.27301
78	133	1254	566823.9	933439.3	37P	1361	144.32801
79	134	1255	567420.9	932500.9	37P	1380	145.42101
80	135	1256	567628.4	931231.7	37P	1637	146.45801
81	136	1257	568495.6	930668.4	37P	1752	147.47401
82	137	1259	570079.1	929371.7	37P	1868	149.51501
83	138	1260	570466.5	928479.8	37P	1938	150.42001
84	139	1261	571310.5	927943	37P	1976	151.39301
85	140	1263	573204.7	926688.2	37P	2110	153.62301
86	141	1264	574362.8	926516	37P	2093	154.56801
87	142	1265	574071.7	925624.6	37P	2109	154.99201
88	143	1267	574049.1	923340.4	37P	2291	156.59201
89	144	1268	573922.3	922188.5	37P	2451	157.33301
90	145	1269	574308.3	921191.4	37P	2529	158.31101
91	146	1271	573053.8	919268.8	37P	2570	158.83701
92	147	1272	572399.4	918500.4	37P	2579	158.95501
93	148	1273	571611.4	917511.7	37P	2576	159.14501
94	149	1275	573494.3	915973.8	37P	2609	161.55501
95	150	1276	574476.6	915932.8	37P	2633	162.25001
96	151	1277	575042.9	914989.2	37P	2613	163.32601
97	152	1279	575905.0	913294.4	37P	2653	165.15801
98	153	1280	576021.8	912312.2	37P	2693	165.96501
99	154	1282	576799.3	910661.2	37P	2704	167.70901
100	155	1283	576512.2	909695.7	37P	2686	168.235

			Geophones Location			OFFSET(Km)	
order	trace	site	easting	northing	zone	ELVA(m)	From SH-13
101	156	1284	576081.6	908722.2	37P	2686	168.67
102	157	1286	577055.7	906860	37P	2682	170.718
103	158	1287	577511.8	905923.7	37P	2672	171.721
104	159	1288	577974.6	905028.2	37P	2663	172.701
105	160	1289	578461.4	904179	37P	2659	173.661
106	161	1291	578876.3	902926.6	37P	2666	174.549
107	162	1292	577933.9	902039.5	37P	2655	174.935
108	163	1293	577174.4	901127.3	37P	2637	175.132
109	164	1294	577639.9	900235.8	37P	2635	176.12
110	165	1295	578112.5	899346.2	37P	2626	177.1
111	166	1297	577593.8	897561.5	37P	2587	178.142
112	167	1298	576431.6	897211.4	37P	2622	177.672
113	168	1300	576204.0	895909.1	37P	2605	178.547
114	169	1302	575675.8	893522.4	37p	2595	180.08
115	170	1303	575681.5	892475.4	37P	2588	180.911
116	171	1304	575432.0	891508.3	37P	2570	181.519
117	172	1305	575746.9	890436	37P	2568	182.558
118	173	1307	576162.5	888738.8	37P	2542	184.161
119	174	1308	575863	887776.2	37P	2531	184.74
120	175	1309	575782.5	886783.5	37P	2506	185.488

Annex-C. Shot Geophone pairs and Offsets

Order	Trace	Site	Elvation(m)	SHOT-13	SHOT-14	SHOT-25	SHOT-16	SHOT-17
1	56	1156	2381	65.189	0.439	-73.429	-122.909	-170.759
2	57	1158	2329	67.019	2.292	-71.61	-121.296	-169.062
3	58	1159	2318	67.867	3.149	-70.768	-120.541	-168.27
4	59	1160	2301	68.688	3.941	-69.928	-119.554	-167.321
5	60	1161	2296	69.278	4.672	-69.329	-118.671	-166.52
6	61	1162	2275	69.926	5.487	-68.693	-117.846	-165.744
7	62	1164	2280	71.016	7.029	-67.671	-116.403	-164.41
8	63	1165	2233	71.799	7.988	-66.936	-115.495	-163.54
9	64	1166	2190	72.599	8.828	-66.164	-114.651	-162.706
10	65	1167	2168	73.696	10.204	-65.169	-113.369	-161.487
11	66	1169	2169	75.442	11.854	-63.458	-111.635	-159.736
12	67	1172	2362	80.616	15.964	-58.131	-109.202	-156.333
13	68	1173	2362	81.614	16.922	-57.1	-108.12	-155.257
14	69	1174	2367	82.569	17.844	-56.109	-107.034	-154.193
15	70	1175	2452	83.475	18.772	-55.237	-106.373	-153.442
16	71	1176	2474	84.33	19.608	-54.361	-105.468	-152.536
17	72	1177	2414	84.516	19.765	-54.108	-104.787	-152.004
18	73	1178	2403	84.626	19.915	-53.982	-104.192	-151.566
19	74	1180	2390	85.824	21.253	-52.844	-102.49	-150.022
20	75	1181	2375	86.822	22.259	-51.857	-101.502	-149.018
21	76	1183	2316	88.717	24.247	-50.039	-99.426	-146.985
22	77	1184	2288	89.684	25.247	-49.109	-98.41	-145.977
23	78	1185	2267	90.609	26.258	-48.272	-97.323	-144.943
24	79	1186	2274	91.597	27.199	-47.259	-96.46	-144.019
25	80	1187	2251	92.501	28.169	-46.436	-95.436	-143.033
26	81	1188	2252	93.062	28.856	-46.022	-94.646	-142.334
27	82	1190	2182	94.637	30.543	-44.631	-92.91	-140.654
28	83	1191	2147	95.654	31.493	-43.569	-92.021	-139.697
29	84	1192	1820	97.936	33.548	-41.055	-90.285	-137.698
30	85	1193	1766	99.044	34.614	-39.914	-89.332	-136.666
31	86	1194	1740	100.089	35.673	-38.911	-88.286	-135.606
32	87	1196	1691	102.19	37.815	-36.931	-86.142	-133.451

Order	Trace	Site	Elvation(m)	SHOT-13	SHOT-14	SHOT-25	SHOT-16	SHOT-17
33	88	1197	1672	103.114	38.755	-36.067	-85.203	-132.507
34	89	1199	1654	104.758	40.28	-34.245	-84.024	-131.101
35	90	1200	1653	105.055	40.486	-33.786	-84.137	-131.037
36	91	1201	1631	105.752	41.131	-33.002	-83.78	-130.528
37	92	1202	1591	106.29	41.629	-32.402	-83.558	-130.169
38	93	1203	1565	107.378	42.719	-31.323	-82.539	-129.099
39	94	1205	1520	109.386	44.735	-29.344	-80.622	-127.101
40	95	1206	1503	110.475	45.832	-28.282	-79.554	-125.999
41	96	1207	1486	111.568	46.93	-27.212	-78.508	-124.909
42	97	1208	1475	112.584	47.949	-26.215	-77.555	-123.906
43	98	1210	1463	114.335	49.829	-24.883	-75.112	-121.723
44	99	1211	1468	115.393	50.952	-24.102	-73.796	-120.505
45	100	1212	1523	116.642	52.195	-22.902	-72.653	-119.288
46	101	1213	1599	117.566	53.092	-21.925	-71.926	-118.449
47	102	1215	1662	119.222	54.704	-20.179	-70.639	-116.955
48	103	1216	1709	119.658	55.201	-20.052	-69.884	-116.339
49	104	1217	1824	120.646	56.231	-19.354	-68.747	-115.253
50	105	1218	1850	121.671	57.256	-18.433	-67.792	-114.241
51	106	1220	1892	122.165	57.936	-19.024	-66.524	-113.357
52	107	1221	1986	123.039	58.847	-18.53	-65.558	-112.426
53	108	1222	2018	123.879	59.687	-17.878	-64.757	-111.589
54	109	1223	2060	124.84	60.637	-17.077	-63.884	-110.652
55	110	1224	1940	126.163	61.954	-16.06	-62.656	-109.349
56	111	1225	1869	127.048	62.854	-15.545	-61.761	-108.443
57	112	1227	1761	127.964	63.904	-15.953	-60.405	-107.321
58	113	1228	1714	128.719	64.71	-15.915	-59.514	-106.499
59	114	1229	1610	129.132	65.235	-16.541	-58.784	-105.956
60	115	1230	1517	129.402	65.616	-17.234	-58.229	-105.58
61	116	1232	1455	130.467	66.911	-18.468	-56.679	-104.352
62	117	1233	1454	131.601	68.091	-18.466	-55.475	-103.192
63	118	1234	1458	132.137	68.511	-17.479	-55.187	-102.72
64	119	1236	1430	133.183	69.345	-15.529	-54.705	-101.845
65	120	1237	1428	133.461	69.504	-14.419	-54.806	-101.7
66	121	1239	1393	134.429	70.305	-12.546	-54.525	-100.983
67	122	1240	1357	134.663	70.458	-11.627	-54.672	-100.902

Order	Trace	Site	Elvation(m)	SHOT-13	SHOT-14	SHOT-25	SHOT-16	SHOT-17
68	123	1241	1321	134.844	70.544	-10.47	-55.005	-100.939
69	124	1243	1283	135.431	71.002	-8.6	-55.305	-100.74
70	125	1244	1295	134.929	70.45	-8.052	-56.138	-101.416
71	126	1245	1266	135.763	71.221	-6.733	-55.965	-100.874
72	127	1247	1269	138.008	73.472	-6.347	-53.973	-98.663
73	128	1248	1281	138.823	74.307	-6.736	-53.075	-97.774
74	129	1249	1295	139.767	75.27	-7.231	-52.073	-96.763
75	130	1250	1300	140.588	76.106	-7.701	-51.227	-95.897
76	131	1251	1312	141.492	77.025	-8.258	-50.319	-94.953
77	132	1253	1339	143.273	78.811	9.208	-48.746	-93.19
78	133	1254	1361	144.328	79.863	9.785	-47.89	-92.177
79	134	1255	1380	145.421	80.968	10.664	-46.854	-91.058
80	135	1256	1637	146.458	82.048	11.922	-45.57	-89.866
81	136	1257	1752	147.474	83.049	12.487	-44.864	-88.934
82	137	1259	1868	149.515	85.075	13.925	-43.345	-87.011
83	138	1260	1938	150.42	85.999	14.868	-42.409	-86.044
84	139	1261	1976	151.393	86.958	15.551	-41.777	-85.159
85	140	1263	2110	153.623	89.161	17.249	-40.362	-83.13
86	141	1264	2093	154.568	90.07	17.791	-40.13	-82.418
87	142	1265	2109	154.992	90.536	18.533	-39.251	-81.775
88	143	1267	2291	156.592	92.223	20.7	-36.968	-79.799
89	144	1268	2451	157.333	93.016	21.775	-35.823	-78.862
90	145	1269	2529	158.311	94.019	22.837	-34.808	-77.811
91	146	1271	2570	158.837	94.695	24.406	-32.967	-76.818
92	147	1272	2579	158.955	94.887	25.039	-32.263	-76.517
93	148	1273	2576	159.145	95.175	25.893	-31.376	-76.124
94	149	1275	2609	161.555	97.549	27.726	-29.644	-73.8
95	150	1276	2633	162.25	98.189	27.975	-29.543	-73.234
96	151	1277	2613	163.326	99.279	29.026	-28.578	-72.135
97	152	1279	2653	165.158	101.145	30.883	-26.871	-70.241
98	153	1280	2693	165.965	101.994	31.865	-25.889	-69.349
99	154	1282	2704	167.709	103.773	33.66	-24.256	-67.542
100	155	1283	2686	168.235	104.366	34.523	-23.28	-66.895
101	156	1284	2686	168.67	104.879	35.366	-22.297	-66.338
102	157	1286	2682	170.718	106.962	37.408	-20.469	-64.246

Order	Trace	Site	Elvation(m)	SHOT-13	SHOT-14	SHOT-25	SHOT-16	SHOT-17
103	158	1287	2672	171.721	107.985	38.428	-19.567	-63.218
104	159	1288	2663	172.701	108.982	39.411	-18.723	-62.218
105	160	1289	2659	173.661	109.955	40.358	-17.943	-61.242
106	161	1291	2666	174.549	110.915	41.547	-16.692	-60.276
107	162	1292	2655	174.935	111.379	42.303	-15.75	-59.823
108	163	1293	2637	175.132	111.681	43.022	-14.756	-59.566
109	164	1294	2635	176.12	112.684	43.995	-13.922	-58.571
110	165	1295	2626	177.1	113.681	44.966	-13.112	-57.584
111	166	1297	2587	178.142	114.862	46.599	-11.267	-56.525
112	167	1298	2622	177.672	114.505	46.719	-10.793	-57.016
113	168	1300	2605	178.547	115.475	47.965	-9.481	-56.185
114	169	1301	2595	180.08	117.198	50.236	-7.086	-54.808
115	170	1302	2588	180.911	118.093	51.274	-6.038	-54.052
116	171	1303	2570	181.519	118.783	52.194	-5.085	-53.552
117	172	1304	2568	182.558	119.861	53.301	-3.997	-52.584
118	173	1305	2542	184.161	121.531	55.043	-2.322	-51.117
119	174	1307	2531	184.74	122.198	55.951	-1.336	-50.702
120	175	1308	2506	185.488	123.015	56.925	-0.344	-50.106

Annex-D. First arrival data used in the analysis

Geophones		Arrival time (millisecond)				
Station	Elvation(m)	SH-13	Sh-14	Sh-25	Sh-16	Sh-17
37.390	2381	11.570	0.194	13.897	21.985	29.295
38.439	2329	11.882	0.685	13.562	21.633	29.232
39.397	2301	12.228	1.187	13.250	21.306	28.734
40.107	2275	12.468	1.748	12.994	20.982	28.310
40.732	2280	12.588	2.308	12.949	20.640	28.211
41.181	2233	12.785	2.528	12.883	20.531	28.160
41.640	2190	12.961	2.729	12.822	20.433	28.059
42.269	2168	13.131	3.034	12.589	20.262	27.771
43.270	2169	13.426	3.431	12.167	20.058	27.564
46.238	2362	14.133	4.161	11.416	19.780	27.007
46.810	2362	14.343	4.342	11.290	19.585	26.728
47.878	2452	14.743	4.609	10.941	19.263	26.388
48.368	2474	14.778	4.688	10.776	18.934	26.218
49.798	2375	15.038	5.074	10.210	17.599	25.455
50.884	2316	15.386	5.511	9.890	17.219	25.269
51.439	2288	15.564	5.698	9.726	16.970	25.139
52.536	2274	15.918	6.048	9.400	16.463	24.925
54.280	2182	16.459	6.667	8.882	16.110	24.345
54.863	2147	16.624	6.719	8.750	16.132	24.139
57.407	1740	17.273	7.416	7.985	15.566	23.448
58.612	1691	17.634	7.742	7.700	14.995	23.117
59.142	1672	17.777	7.853	7.591	14.731	23.055
60.085	1654	18.108	8.168	7.367	14.605	22.990
60.255	1653	18.145	8.309	7.279	14.659	22.876
60.655	1631	18.239	8.416	7.193	14.690	22.829
60.964	1591	18.317	8.423	7.127	14.881	22.722
61.588	1565	18.472	8.590	6.857	14.734	22.515
63.991	1486	19.145	9.443	6.285	13.987	21.863
64.574	1475	19.309	9.613	6.164	13.774	21.715
66.901	1523	20.167	10.290	5.419	13.205	21.148
68.631	1709	20.746	10.821	4.887	12.954	20.798
70.069	1892	20.978	11.386	4.557	12.121	20.441
71.603	2060	21.485	12.022	4.318	11.085	20.167
73.395	1761	22.009	12.815	4.079	10.523	19.711
73.828	1714	22.157	12.497	4.051	10.362	19.548
74.065	1610	22.317	12.479	4.166	10.263	19.432
74.831	1455	22.487	12.884	4.521	10.242	19.046
75.481	1454	22.729	12.970	4.453	10.112	18.804
75.788	1458	22.765	12.949	4.299	10.153	18.677

Geophones		Arrival time (millisecond)				
Station	Elvation(m)	SH-13	Sh-14	Sh-25	Sh-16	Sh-17
76.388	1430	22.985	13.158	3.986	9.970	18.527
77.237	1357	23.367	13.395	3.108	9.703	18.303
79.623	1281	23.987	14.218	1.964	9.524	17.607
80.165	1295	24.136	14.484	2.057	9.410	17.447
80.636	1300	24.158	14.639	2.352	9.322	17.303
81.154	1312	24.196	14.794	2.512	9.258	17.133
86.833	1976	25.626	16.341	4.228	7.577	15.470
88.112	2110	26.016	16.572	4.477	7.265	15.112
90.240	2451	26.679	17.148	5.140	6.592	13.974
91.170	2579	26.796	17.360	5.707	6.082	13.653
91.279	2576	26.645	17.530	5.782	5.956	13.630
92.661	2609	27.057	17.804	6.087	5.706	13.914
93.060	2633	27.178	17.850	6.152	5.697	13.763
95.191	2653	27.405	18.252	6.522	5.059	12.828
96.493	2704	27.831	18.614	6.930	4.532	12.349
96.742	2686	27.918	18.682	7.061	4.335	12.198
98.492	2682	28.303	19.215	7.473	4.075	11.746
99.054	2672	28.438	19.422	7.621	4.091	11.591
99.605	2663	28.701	19.528	7.774	3.962	11.433
100.114	2659	28.959	19.599	7.896	3.809	11.243
100.336	2666	29.039	19.728	8.061	3.521	11.177
100.448	2637	29.068	19.796	8.250	3.186	11.049
102.174	2602	29.597	20.836	9.407	1.583	10.218
103.760	2588	29.745	20.621	9.512	1.347	10.159
103.763	2570	29.855	20.858	9.733	0.984	10.094
104.112	2568	30.835	20.886	9.907	0.711	10.008
104.708	2542	30.274	21.649	10.049	0.387	9.726

Annex-E. Subsurface information obtained from the analysis

		LAYER VELOCITY(in m/sec)				REFRACTOR DEPTH(Km)		
No.	station	V1	V2	V3	V4	Z1	Z2	Z3
1	37.39							
2	38.44	2832.0				1.54		
3	39.40		3396.48	5434.38			3.22	
4	40.11	2950.0	3396.48	5434.38		1.55	3.33	
5	40.73		3396.48	5434.38			3.26	
6	41.18	2950 .0				1.55		
7	41.64	2950.0	3396.48	5717.94		2.00	3.15	
8	42.27							
9	43.27		3396.48	4494.22	6295.88		2.94	9.44
10	46.24		3396.48	4494.22	6295.88		3.00	10.2
11	46.81		3396.48	4494.22	6295.88		2.96	9.5
12	47.88	2834.58		4494.22	6295.88	1.88		10.0
13	48.37		3396.48	4494.22	6295.88		2.99	10.9
14	48.53	2834.58			6295.88	1.78		11.6
15	49.80		3396.48	4494.22			3.11	
16	50.88		3396.48		6295.88		2.93	8.5
17	51.44			4494.22	6295.88			10.3
18	52.54	2780.0	3396.48			1.94	3.02	
19	54.28			4494.22				
20	54.86		3396.48	4494.22	6455.88		2.79	6.8
21	57.41	2750.0	3396.48		6455.88	1.69	2.74	6.25
22	58.61		3396.48		6455.88		2.84	7.56
23	59.14	2800	3396.48			1.78	2.87	
24	60.08						2.84	
25	60.26							
26	60.66							
27	60.96	2500.0		4494.22	6455.88	2.2		6.5
28	61.59		3396.48	4494.22			3.76	
29	63.99	2550.0	3396.48	4494.22		2.06	3.71	
30	64.57		3396.48	4494.22			3.79	
31	66.90	2500.0	3396.48	4494.22		2.49	3.88	
32	68.63		3396.48	4494.22			4.23	
33	70.07		3396.48	4494.22	6295.88		4.84	8.76
34	71.60		3396.48	4494.22	6295.88		4.46	9.32
35	73.39		3396.48	4494.22	6295.88		3.83	9.52
36	73.83							
37	74.06		3396.48	4494.22	6295.88		3.74	10.41
38	74.83		3396.48	5744.14			3.81	

		LAYER VELOCITY (in m/sec)				REFRACTOR DEPTH (Km)		
No.	station	V1	V2	V3	V4	Z1	Z2	Z3
39	75.48							
40	75.79		3396.48	5486.76			2.74	
41	76.39	2550.0		4494.22	6295.88	1.5		10.48
42	77.24	2750.0	3396.48	4494.22	6299.51	1.5	3.73	9.33
43	79.16	2600.0	3396.48	5486.76		3.4	4.07	
44	79.62	2600.0	3396.48	5784.14		1.75	3.84	
45	80.16	2600.0				1.6		
46	80.64							
47	81.15			4494.22	6303.13			8.23
48	86.83		3396.48	4494.22	6303.13		4.18	7.98
49	88.11		3396.48	4494.22	6303.13		4.16	7.62
50	90.24		3396.48	4494.22	6303.13		4.89	7.31
51	91.17		3396.48				4.66	
52	91.28		3396.48				4.53	
53	92.66			4494.22				
54	93.06		3396.48	4494.22			3.54	
55	95.19		3396.48	4494.22	6303.13		3.97	6.36
56	96.49				6303.13			6.45
57	96.74		3396.48	4494.22	6303.13		3.49	6.18
58	98.49		3396.48	5201.66			3.15	
59	99.05		3396.48	4761.64			3.51	
60	99.60							
61	100.11	3250				1.8		
62	100.34					1.44		
63	100.45	3000.0	3396.48	4761.64			3.98	
64	102.17		3396.48	4761.64			4.38	
65	103.76	3200.0	3396.48	4761.64		1.5	4.44	
66	103.76							
67	104.11	3272.0				1.44		
68	104.71							

DECLARATION

I , the undersigned, herby declare that this thesis is my original work carried out under the supervision of Dr. Tilahun Mammo, has not been presented as a thesis for a degree program in any other University and that all sources of the materials used are duly acknowledged.

NAME Mehari Melak

SIGN. _____

DATE 14/07/04

This thesis has been submitted for the examination with my approval as his advisor;

Dr. Tilahun Mammo

Sign: _____

Date 15.07.04

Date and place of submission;

School of Graduate Studies,

June 2004.